Article

Not peer-reviewed version

The Finite-Size Nuclear Structure of the Black Hole

Ting-Han Pei *

Posted Date: 12 July 2024

doi: 10.20944/preprints202109.0354.v2

Keywords: black hole; Schwarzschild radius; Kerr-Newman metric; geodesic; finite-size nuclear structure

Article

The Finite-Size Nuclear Structure of the Black Hole

Ting-Han Pei [1,2]

[1] Institute of Astronomy and Astrophysics, Academia Sinica, Taipei, Taiwan; 157328@mail.fju.edu.tw or Thpei142857@gmail.com
[2] Department of Electrical Engineering, Fu Jen Catholic University, New Taipei City, Taiwan

Abstract Although some alternative metrics have been proposed in classical gravity, the singularity problem remains unresolved perfectly. To satisfy the super-gravitational requirement of a black hole without singularities, we propose some possible finite-size structure to avoid the confused one. In this research, the degenerate Fermi electron gas is first used to reveal that the Fermi electron gas cannot shrink to a point regardless of how much energy it obtains; therefore, the singularity existing at the center becomes very unreasonable. To avoid these problems, a finite-size nucleus of the black hole is proposed and explained by the behaviors of the Fermi electron gas and Fermi neutron gas for this finite-size nuclear model. We construct the Kerr-Newman black hole by using a non-rotating but charged finite-size nucleus, a compact-like star, which is surrounded by counter-rotating and corotating electrons. Based on this model, the super-gravity the same as the one from a black hole is presented, and the speed of light observed at far-away places can be nonzero at the event horizon.

Keywords: black hole; Schwarzschild radius; Kerr-Newman metric; geodesic; finite-size nuclear structure

PACS: 95.30.-k –Fundamental Aspects of Astrophysics; 98.80.JK –Mathematical and Relativistic Aspects of Cosmolog

1. Introduction

Some candidates of the black holes have been found for many years [1-3]. Although we don't know what the structure inside the black hole is, we can make sure that there is some heavy mass gathering in a small space which we call the outer boundary, the event horizon, of the black hole. For a long time, the center of a black hole is thought as a singularity and all mass as well as all charges gather there. The massive particles, even light, cannot escape the black hole due to ultra-strong gravity. But is it true for light or a photon such as a massless particle? As we know, recent observation shows that a black hole fast moves in one direction and leaves a trajectory including many stars in formation in space [4]. It reveals that such a black hole shall have an inner heavy finite structure to generate super-gravitational fields around it. The zero dimension of the singularity inside a black hole seems to be unable to explain such a phenomenon.

Recently, gravitational waves from the mergers of binary black holes have been revealed by LIGO and VIRGO several times [5-8]. Because the mass of each black hole exists within each event horizon, the merger means that two event horizons have to intersect with each other, then their mass can merge, and finally, several equivalent solar-mass energy was released to space. Actually, the mass of the new black hole is less than the summation of the two original black holes. A problem is where does the lost mass go? It is just the merger causing a collision between the two black holes and then resulting in mass loss. The lost mass is transferred to other forms such as the gravitational wave and electromagnetic wave. These mergers seem to reveal that gravitational waves were from the collisions of inner structures of two black holes. Due to the variation of the total mass, the spacetime structure outside the new black hole is also different from that of the two black holes before the merge. If the gravitational wave is confined in the black hole, the black hole behaves like a closed system and the spacetime structure outside it cannot change without the gravitational wave delivering some information about the variation of mass inside the black hole. In addition, the other observation from

 doi:10.20944/preprints202109.0354.v2

a binary neutron star showed both receiving signals of gravitational waves and electromagnetic waves almost at the same time [9]. Since gravitational waves and electromagnetic waves originate from the same black hole and both follow the null geodesic in the same spacetime structure, we might ask why the gravitational wave can leave the black hole, but light cannot.

On one hand, the singularity has a nonphysical infinite density in mass, charge, and energy there; on the other hand, the mergers of two black holes also imply the inner structure of the black hole to be a very high-density nucleus. It gives rise to a curiosity about whether this singularity is reasonable in a black hole or not. In this research, we first discuss this topic from the characteristics of light at the black hole. Then we consider energy conservation applied to a black hole and its previous star to propose a finite-size nucleus in the black hole and discuss the limitation of nuclear size. Finally, the discussion of the radial speed of light predicts the expansion of the black hole to be observable.

2. The Velocity Of Light In The Schwarzschild Black Hole

Before obtaining deeper perspectives about the structure of the black hole, first, we discuss something interesting that light propagating from outer space, passes through the event horizon, into the non-rotating and uncharged black hole with a Schwarzschild radius $R_S=2GM/c^2$, where M is the mass of the black hole, c is the speed of light in free space, and G is the gravitational constant. This discussion is easy to examine whether such a kind of black hole theory can be further improved or not. Its spacetime structure is described by the Schwarzschild metric and there is one event horizon for this kind of black hole. The Schwarzschild metric [10-15] in the spherical polar coordinate $(r,\ \theta,\ \phi)$ and the coordinate time t is expressed as

$$\mathrm{d}s^2 = e^{\nu(r)}c^2\mathrm{d}t^2 - e^{\lambda(r)}\mathrm{d}t^2 - \mathrm{d}\theta^2 - r^2\sin^2\theta\mathrm{d}\phi^2 = c^2\left(1-\frac{R_S}{r}\right)\mathrm{d}t^2 - \left(1-\frac{R_S}{r}\right)^{-1}\mathrm{d}r^2 - \mathrm{d}\theta^2 - r^2\sin^2\theta\mathrm{d}\phi^2, \qquad (1)$$

where the coordinate time t in a gravitational field is the time read by the clock stationed at infinity because the proper time and coordinate time become identical there [14]. Then we derive the propagation equation of light in this metric. Light propagates along the null geodesic with $\mathrm{d}s^2=0$, and the velocity of light in the Schwarzschild metric has been obtained [10-13] which is

$$\frac{1}{\left(1-\frac{R_S}{r}\right)^2}\left(\frac{\mathrm{d}r}{\mathrm{d}t}\right)^2 + \frac{1}{1-\frac{R_S}{r}}\left(r\frac{\mathrm{d}\theta}{\mathrm{d}t}\right)^2 + \frac{1}{1-\frac{R_S}{r}}\left(r\sin\theta\frac{\mathrm{d}\phi}{\mathrm{d}t}\right)^2 = c^2. \qquad (2)$$

Considering light propagating along the radial direction with the radial velocity v_r, that is,

$$v_r^2 = \left(\frac{\mathrm{d}r}{\mathrm{d}t}\right)^2 = \left(1-\frac{R_S}{r}\right)^2 c^2. \qquad (3)$$

It gives $v_r=0$ at $r=R_S$ where light has to spend infinite time passing through or leaving away from the event horizon. Because all our observations proceeded on the Earth, we have to use the viewpoint of a far observer, to predict what we should "see" on the Earth according to the Schwarzschild metric or the black hole theory. Then considering a test massive particle, the spending time from r_0 to R_S observed by a far observer on the Earth is [13]

$$\int_{r_0}^{R_S}\mathrm{d}t = \frac{A}{c}\int_{r_0}^{R_S}\frac{1}{\left(1-\frac{R_S}{r}\right)\sqrt{A^2-\left(1-\frac{R_S}{r}\right)}}\mathrm{d}r = \infty, \qquad (4)$$

where A is a constant between 0 and c. The integral in Equation (4) gives the infinitely spending time from a finite distance r_0 to R_S. Therefore, the Schwarzschild metric or the black hole theory predicts that from the viewpoint of a far observer on Earth, nothing can enter the black hole even if he can wait 30 billion years, which is predicted by the black hole theory. Clearly speaking, it results in nothing passing through the event horizon into the black hole in finite time, in the viewpoint of observations on Earth far away from the black hole. Furthermore, according to the infinite redshift of light rays at the event horizon, it would even be unlikely to see any variation in the black hole because no light information can be detectable from the event horizon. However, this might induce a problem.

 doi:10.20944/preprints202109.0354.v2

Recently, the Event Horizon Telescope (EHT) has shown images about the accretion disk of the M87 black hole [16]. The expansion and seeds of black holes are also reported [17-19]. Therefore, the issue, of whether the nowadays black hole theory can explain the expansion of a black hole or not, is raised.

If the gravity of the black hole doesn't change during the light propagation, Equation (3) tells us that the radial speed of light has two solutions with the same value but different signs at the outer event horizon [20]: one is into the black hole and the other is away from the black hole. Furthermore, the light should not stop at the event horizon and continuously propagate across the event horizon. If the gravitational wave is confined in the black hole, the black hole seems to behave like a closed system because no gravitational wave can deliver some information from the inside of the black hole. More detailed, for the radial light or a radial photon, its trajectory is along a radial direction and described by $ds^2=0$. Then its velocity is expressed in Equation (3) and the coordinate time t and the proper time τ taken from r_0 to r ($r_0>r\geqq R_S$) are respectively

$$t(r)=\int_{r_0}^{r}\frac{1}{c\left(1-\frac{R_S}{r}\right)}\mathrm{d}r=\frac{r_0-r}{c}+\frac{R_S}{c}\ln\left(\frac{r_0-R_S}{r-R_S}\right), \tag{5}$$

and

$$\begin{aligned}\tau(r)&=\int_{r_0}^{r}\frac{1}{c\left(1-\frac{R_S}{r}\right)^{1/2}}\mathrm{d}\tau\\&=\left[\frac{r_0}{c}\left(1-\frac{R_S}{r_0}\right)^{1/2}-\frac{r}{c}\left(1-\frac{R_S}{r}\right)^{1/2}\right]+\left(\frac{R_S}{c}\right)\ln\left[\frac{r_0^{1/2}+(r_0-R_S)^{1/2}}{r^{1/2}+(r-R_S)^{1/2}}\right].\end{aligned} \tag{6}$$

Actually, the τ-r relation in Equation (6) is also suitable for describing the radial photon inside the event horizon keeping in a fixed direction towards the center of the black hole. Therefore, for $\tau(r)$, the τ-r curve is continuous through $r=R_S$, and light or a photon spends a finite proper time across the event horizon.

Therefore, when we describe the spacetime structure in the vicinity of a black hole, it has a problem to explain the expansion of the black hole. Furthermore, the speed of light at $r\leq R_S$ is also unreasonable. According to these, we try to use another metric to solve these problems in this paper.

3. The Physical Finite-Size Nucleus Model In The Black Hole

3.1. A Charged Sphere With A Radius Of Fifty Meters And The Universal Energy

In this following, we propose new perspective for the black hole to start solving the above problems, by discussing the physical viewpoint on the structure of the black hole based on electrons and nuclear physics. All the above-mentioned research [21-29] is deduced from the mathematical viewpoint without any physical assumptions of material structures. If we review the evolution of a star at the final stage, it tells us that the star could become a white dwarf star, neutron star, or black hole, dependent on its initial mass. In 1931, Chandrasekhar used special relativity and quantum statistical thermodynamics to give a non-rotating star with a mass limit of 1.4 $M_\odot$ (Chandrasekhar limit) due to electron-gas degenerate pressure [30,31]. Such a star is called a white dwarf star, which will collapse into a neutron star if its mass is slightly more massive than the Chandrasekhar limit [32]. This kind of neutron star was predicted to collapse further when its mass is exceeding this limit. But in 1939 and later, Oppenheimer and others, only based on the Pauli exclusion principle and neutron-neutron repulsion, the first predicted that neutron stars to have another mass limit of approximately 0.7 $M_\odot$ (the Tolman–Oppenheimer–Volkoff limit) [32-34]. However, at that time, nuclear physics only considered Coulomb's and nuclear forces between neutrons, protons, and electrons, without strong interaction and any inside structures such as quarks and gluons. Until now, the collapse of a star to a black hole still accords to the thoughts one century ago. Before collapse to a smaller size, the physical laws remain useful and therefore, we have to and are unavoidable to consider energy

 doi:10.20944/preprints202109.0354.v2

conservation to see whether the collapse can be continuous to a singularity, or eventually stop at a certain size. Due to the new physics such as strong interaction, developed after the 1940s, we propose another way to emphasize the finite-sized nuclear structure inside the black hole. The real material structure allows us to consider this viewpoint. Recently, the proton experiments [35] showed the inside pressure of the proton as high as 10^{35} Pascals, and it is almost 10 times as large as the core pressure of a traditional neutron star. Such strong pressure indicates a great ability for the proton to bear the gravitational squeeze. Therefore, gravity collapse is so doubtful to reconsider the internal structure of the black hole. A report reveals the equivalent mass-energy of the observable universe is about $1.3\text{x}10^{70}$ J [36]. Theoretically speaking, the Coulomb's interaction shows a lot of necessary work done to for charges to form a charged sphere. Let us consider a case where $1.4\text{x}10^{31}$ Coulomb (C) electrons to form a sphere. So many electrons have mass of $7.96\text{x}10^{19}$ kg. If these electrons are gathered from infinity to form a sphere with a radius of 50 meter, as shown in Figures 1(a) and 1(b), then the mass density is $1.52\text{x}10^{14}$ kg/m^3, which is within the density range of a white dwarf star, in which the inside pressure is supported by the degenerate pressure of the Fermi electron gas. According to the description in the Feynman Lectures Volume II [37], the inverse-square law of the Coulomb force is still a good approximation when the distance between two charges is as small as 10^{-15} meter. In our case, the distance between two electrons is $2.25\text{x}10^{-15}$ meter, which is larger than the criterion of 10^{-15} meter. Thus, the self-energy of our case can be still appropriately calculated by the classical electrodynamics. Here we consider the additional charged case that the Coulomb's interaction is calculated. The Reissner–Nordström metric for the exterior geometry is defined by [38-41]

$$ds^2 = c^2\left(1-\frac{2GM}{c^2r}+\frac{KGQ^2}{c^4r^2}\right)dt^2-\left(1-\frac{2GM}{c^2r}+\frac{KGQ^2}{c^4r^2}\right)^{-1}dr^2-d\theta^2-r^2\sin^2\theta d\phi^2. \quad (7)$$

By adopting the gravitational mass function M of a homogeneous star in the Reissner-Nordström metric, it gives [39,42,43]

$$\frac{2GM}{c^2r}=1-e^{\nu}+\frac{KGQ^2}{c^4r^2}, \quad (8)$$

where Q is the total charge and e^{ν} is one metric potential similar to that in Equation (1). Therefore, to move $1.4\text{x}10^{31}$ Coulomb electrons into a one-meter-radius sphere from infinity one needs to do the work against Coulomb's repulsive interaction for establishing the self-energy which approximates [44]

$$E_{self}=\left(\frac{K}{G}\right)^{1/2}\int_0^R 4\pi c^2\rho_e(r)\frac{\left[e^{\nu(r)}-1+\left(\frac{2GM}{c^2r}\right)\right]^{1/2}}{2}dr$$

$$\cong\int_0^R\frac{K[4\pi r^2\rho_e(r)dr]}{r}\int_0^r 4\pi r'^2\rho_e(r')dr'$$

$$\cong\frac{3}{5}\frac{(8.987\times10^9)(1.4\times10^{31})^2}{50}=2.114\times10^{70}\,J, \quad (9)$$

where the mass term can be ignored and the charge density ρ_e is constant throughout the charged sphere. Thus, even if we use all the observable energy of the universe, theoretically speaking, we cannot shrink $1.4\text{x}10^{31}$ Coulomb electrons to a smaller space even a single point. As we know, a black hole cannot obtain so much energy before collapse or compressing everything into a singularity. Thus, in this case, the black hole has a finite-sized nucleus. The result is possibly used for the charged star.

Preprints.org (www.preprints.org) | NOT PEER-REVIEWED | Posted: 12 July 2024 doi:10.20944/preprints202109.0354.v2

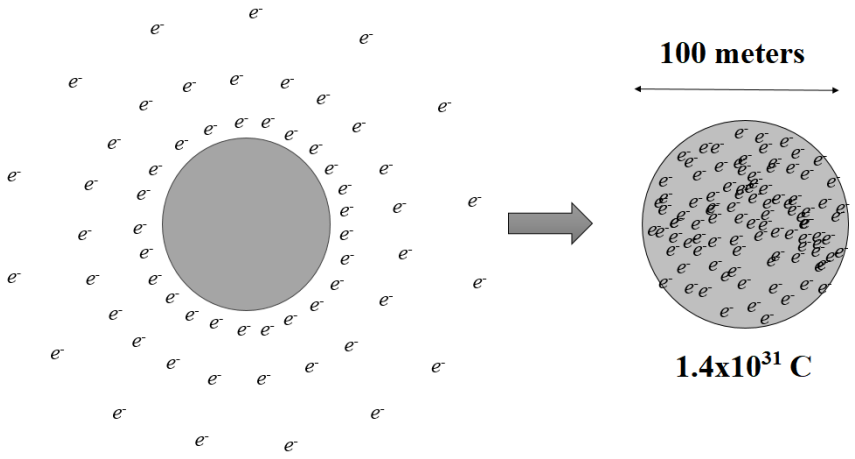

Figure 1. (a) A lot of electrons are moved together from infinity. (b) 1.4x10^{31} C electrons gathering to form a sphere with a radius of 50 meter. It needs energy more than 10^{70} J, which is the total energy in the observable universe or the energy since the birth of the universe.

3.2. A Neutral White Dwarf Star Consisting Of Fermi Electron Gas

Since a lot of black holes are evolutionary from stars with totally finite energy, the initial black hole should also have finite energy. Theoretically speaking, the black hole should have a finite-size nucleus in it. Here we adopt the part of the white dwarf model at absolute zero temperature where N Fermi electrons and $N/2$ helium nuclei coexist at the final stage of a superstar to prove it [45,46]. The volume of the star with a radius of R_0 is

$$V_0 = \frac{4}{3}\pi R_0^3, \tag{10}$$

and the total mass of the star is

$$M \approx (m_e + 2m_n)N \approx 2m_n N, \tag{11}$$

where m_e is the electron mass and m_n the neutron mass. Then at temperature T=0 K, the total kinetic energy of the Fermi electron gas in the ultra-relativistic condition is [46]

$$U_e \approx \frac{2\pi V_0 m_e^4 c^5}{h^3}\left(\frac{p_f}{m_e c}\right)^4 = \frac{2\pi V_0 p_f^4 c}{h^3} = \frac{3Nhc}{4}\left(\frac{3N}{8\pi V_0}\right)^{1/3} = \frac{3}{4}Ncp_f, \tag{12}$$

where the momentum of the Fermi electron is

$$p_f = h\left(\frac{3N}{8\pi V_0}\right)^{1/3}. \tag{13}$$

The total kinetic energy of helium nuclei is almost zero because they are Boson gas to be able to occupy the same lowest-energy state. The total energy of the star without Coulomb's energy at the final stage is

$$U_{total} \approx U_e + Nm_e c^2 + 2Nm_n c^2 + U_g$$

$$\approx \frac{3Nhc}{4}\left(\frac{3N}{8\pi V_0}\right)^{1/3} + Nm_e c^2 + 2Nm_n c^2 + U_g, \tag{14}$$

where the gravitational mass function M of a homogeneous star is [39,42,43]

$$\frac{2GM}{c^2 r} = 1 - e^{-\lambda} + \frac{KGQ^2}{c^4 r^2}, \tag{15}$$

 doi:10.20944/preprints202109.0354.v2

where $e^{-\lambda}$ is one metric potential in the Reissner-Nordström metric. Therefore, for the uncharged case of Q=0, the self-energy calculated by considering an inhomogeneous star with a radius of R is

$$U_g = \int_0^R 4\pi c^2 \rho(r) \frac{\left[1 - e^{-\lambda(r)}\right]}{2} dr = \int_0^R \frac{G[4\pi r^2 \rho(r) dr]}{r} \int_0^r 4\pi r'^2 \rho(r') dr'. \quad (16)$$

For the homogeneous white dwarf star, the above equation gives

$$U_g = \frac{3GM^2}{5R} \approx \frac{3G(2m_n N)^2}{5} \left(\frac{4\pi}{3V_0}\right)^{1/3}. \quad (17)$$

In the later, we will use energy conservation to discuss whether the singularity model in the black hole is reasonable or not.

3.3. The Possible Black-Hole Solutions Of The Nuclear Matter

Next, we consider one negatively charged case again where some Fermi electron gas exists at the center of the black hole to check whether it could be a singularity at the center or not. It means negative charges are more than positive ones, and one situation is that the center consists of some neutral part and the Fermi electron gas. Equation (12) tells us that U_e has infinite energy when V_0 is close to zero. However, electron gas cannot become a singularity point because it needs infinite energy revealed by Equation (8). When to discuss the gravitational collapse [10,11,13], the Fermi electron gas is a good example to check whether the gravitational collapse is reasonable or not [47].

Then we use a neutron star to discuss another possibility to form a black hole. Due to the supernova producing ultra-high pressure, most electrons and protons are supposed to react to turn into neutrons. After that, 2N neutrons theoretically exist there. General Relativity is important in the high-density regions of the white dwarf and neutron stars. Considering the spherically symmetric metric, the general relativistic equations of hydrostatic equilibrium are the Tolman-Oppenheimer-Volkoff (TOV) form [31,48-53],

$$\frac{dp(r)}{dr} = -\frac{G}{r^2}\left[\rho(r) + \frac{p(r)}{c^2}\right]\left[m(r) + 4\pi r^3 \frac{p(r)}{c^2}\right]\left[1 - \frac{2Gm(r)}{rc^2}\right]^{-1}, \quad (18)$$

and

$$\frac{dm(r)}{dr} = 4\pi r^2 \rho(r). \quad (19)$$

When discussing the neutron star, neutrons are the main roles. Theoretical studies of pure neutron matter derived from the nuclear many-body problem using two and three-body potentials fitted to laboratory measurements of nuclear properties by experimental nucleon-nucleon (NN) scattering data, give the density of nuclear matter inside a large nucleus like ^{208}Pb ~ n_s=0.16 nucleon/fm^3 or ρ_s=2.7x10^{14} g/cm^3 [33,51-53]. Based on these values, neutron stars with densities are estimated that up to ~ 7ρ_s [33]. However, it even reveals a prediction of the central pressure close to 625 MeV/fm^3 when the central density approximates 8.5ρ_s calculated by the hadronic equation of state (EOS) [33]. This central pressure value is equal to 10^{35} Pascals, which is the same as the inside pressure of the proton experimentally reported [35]. Therefore, we can expect the central density of a neutron star at least to be 8.5ρ_s by considering the pressure equilibrium. On the other hand, it is reported that one demonstration of the hadronic EOS is consisting of two polytropes (i.e., p=$p_0\rho^\gamma$) [33], where γ is the polytropic exponent, also called the adiabatic index [54]. The two exponents γ_1=4/3, valid for the nuclear matter at densities below ρ_s/3, and γ_2=3 are connected at the transition pressure p_t=p_n/8 and baryon density ρ_s/2, where the pressure p_n=250 MeV/fm^3=10$^{35.8}$ dyne/cm^2 [33]. According to these best-fit EOS parameters, it results in scaling between radius R and mass M as follows

 doi:10.20944/preprints202109.0354.v2

$$R \propto p_0^{1/(3\gamma-4)} M^{(\gamma-2)/(3\gamma-4)} \tag{20a}$$

or

$$M \propto p_0^{1/(\gamma-2)} R^{(3\gamma-4)/(\gamma-2)}. \tag{20b}$$

If the proportional constant K is considered in Equation (20b), mathematically speaking, it will give possible conditions that this neutron star becomes a black hole at R=R_S. Then the R equation satisfying R=R_S is given by

$$R_S = \frac{2GKp_0^{1/(\gamma-2)} R_S^{(3\gamma-4)/(\gamma-2)}}{c^2}. \tag{21a}$$

or

$$R_S = p_0^{-(2\gamma-2)} \left(\frac{c^2}{2GK}\right)^{(\gamma-2)/(2\gamma-2)}. \tag{21b}$$

Explicitly, this expression reveals R_S dependent on the proportionality of K and γ, and has a singularity at γ=2 which shall be avoided and unused. When γ is determined, the smaller K is, the larger R_S. Except for this, there is another division using three-polytropic pieces to fit a fixed-region EOS [52-54]. In this piecewise-polytropic EOS, each piece is specified by two parameters including the density ρ_i and the polytropic exponents γ_i for i=1,2, and 3 [52-54]. These six parameters plus the core-crust transition density ρ_0 are a total of seven parameters used in this fitting EOS [52]. In these pieces, the pressure p and energy density ε is continuous everywhere and the pressure and energy density within $\rho_i \geqq \rho \geqq \rho_{i-1}$, for i=1-2, and $\rho \geqq \rho_{i-1}$, for i=3, satisfy [52-54]

$$p(\rho) = p_i \left(\frac{\rho}{\rho_i}\right)^{\gamma_i} \tag{22}$$

and

$$\varepsilon = \frac{p}{\gamma_i - 1} + \left(\varepsilon_{i-1} - \frac{p_{i-1}}{\gamma_i - 1}\right)\frac{\rho}{\rho_{i-1}}, \tag{23}$$

where

$$\gamma_i = \frac{\ln(p_i/p_{i-1})}{\ln(\rho_i/\rho_{i-1})}. \tag{24}$$

A good fit is found for three polytropic pieces with fixed divisions at ρ_1=1.85ρ_s and ρ_2=2ρ_1=3.70ρ_s [54]. The third density boundary ρ_3 is chosen to be 2ρ_2 [52,54]. Because ρ_0<ρ_1 is required in this polytropic-piecewise EOS, the value ρ_0=2x10^{14} g/cm^3 is chosen as the first density parameter in the same reference [53]. There is another choice of ρ_0 to be ρ_s/2.7 or 10^{14} g/cm^3 [52]. The corresponding p_1, p_2, and p_3 for the EOS FPS are 10$^{34.283}$, 10$^{35.142}$, and 10$^{35.925}$ dyne/cm^2, respectively [53]. The other parameters for the EOS AP3 are 10$^{34.392}$, 10$^{35.464}$, and 10$^{36.452}$ dyne/cm^2, respectively [53]. Using these parameters, three polytropic exponents can be calculated for three polytropic pieces by applying Equation (24). Actually, not only $npe\mu$ matter has been discussed, but also hyperons, pions, Kaon condensate, and quark matter have also been shown the parametrized EOSs [53]. All the candidate EOSs perform very close to trends even some of them crisscross each other as shown in Figure 2. Because the central pressure can be as high as 10^{35} Pascals or 625 MeV/fm^3, the corresponding central mass density is 8.5ρ_s at least. The three-polytropic EOS is bound by ρ_3=2ρ_2=7.4ρ_s which is below our requirement. The ρ-p relation is even considered the central density of 20ρ_s [51]. Therefore, for simplicity, we adopt a unified model to describe the polytropic EOS for the neutron star as the red line plotted in Figure 2, and it can extend to ρ>9ρ_s=2.43x10^{15} g/cm^3. This polytropic EOS has the form

$$\log p - \log p_0 = \frac{4.2}{1.5}(\log \rho - \log \rho_0) \tag{25}$$

or

Preprints.org (www.preprints.org) | NOT PEER-REVIEWED | Posted: 12 July 2024 doi:10.20944/preprints202109.0354.v2

$$p = p_0 \left(\frac{\rho}{\rho_0}\right)^{2.8}, \tag{26}$$

where $\rho_0=\rho_s/2.7=10^{14}$ g/cm^3 and $p_0=10^{32.7}$ dyne/cm^2=0.2485 MeV/fm^3. In addition, the γ=3 polytropic EOS is denoted by the yellow line [51].

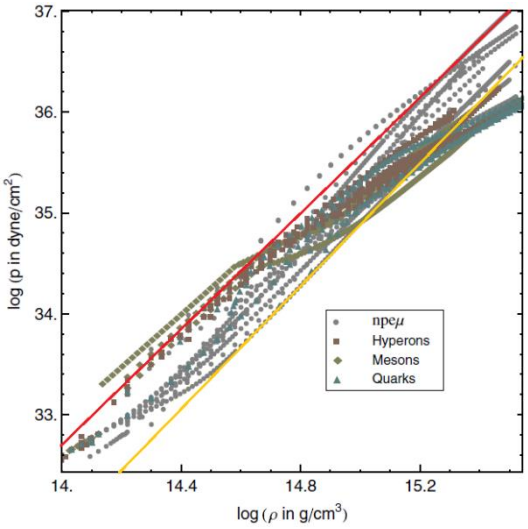

Figure 2. Pressure versus rest mass density for the set of candidate EOSs containing *npeμ* matter, hyperons, pion, Kaon condensates, and quark matter [53]. All these EOSs are performed close to each other and even some EOSs are crisscrossed. For simplicity, we adopt a unified model to represent the *p*-ρ relation for the neutron star which is drawn by the red line. The yellow line is for the γ=3 polytropic EOS.

From Equation (26), it gives

$$\frac{d\rho(r)}{dr} = -\left(\frac{dp}{d\rho}\right)^{-1} \frac{G}{r^2} \frac{\left[\rho(r) + \frac{p(r)}{c^2}\right]\left[m(r) + 4\pi r^3 \frac{p(r)}{c^2}\right]}{\left[1 - \frac{2Gm(r)}{rc^2}\right]}. \tag{27}$$

Equation (27) can be solved numerically as long as the central density is given. On the other hand, substituting Equation (26) into Equation (18) directly gives the *m*-ρ relation

$$m(r) = \left\{ \frac{\left[\rho(r) + \frac{p_0}{c^2}\left(\frac{\rho(r)}{\rho_0}\right)^{\gamma}\right]}{\gamma \frac{p_0}{\rho_0}\left(\frac{\rho(r)}{\rho_0}\right)^{\gamma-1}\left(\frac{d\rho(r)}{dr}\right)} 4\pi r \frac{p_0}{c^2}\left(\frac{\rho(r)}{\rho_0}\right)^{\gamma} + \frac{1}{G} \right\} r^2, \tag{28}$$

$$\frac{2r}{c^2} - \left[\frac{\rho(r) + \frac{p_0}{c^2}\left(\frac{\rho(r)}{\rho_0}\right)^{\gamma}}{\gamma \frac{p_0}{\rho_0}\left(\frac{\rho(r)}{\rho_0}\right)^{\gamma-1}\left(\frac{d\rho(r)}{dr}\right)}\right]$$

where γ=2.8. Because $(d\rho/dr)< 0$ in the neutron star, the denominator is positive. Once $d\rho/dr$ in Equation (27) is obtained, then $m(r)$ in Equation (28) can be calculated where $\rho(r)$ is evaluated by iteration based on the finite-difference method. In our simulations, the radial difference Δr of 10^{-3} meter is used for calculations. This Δr is sufficiently convergent that the calculations of $\Delta r=10^{-1}$ are almost the same as those of $\Delta r=10^{-3}$. If the condition

$$r \le \frac{2Gm(r)}{c^2} = R_S(r) \tag{29}$$

 doi:10.20944/preprints202109.0354.v2

is satisfied, then the neutron star can be treated as a non-rotating and uncharged black hole with a radius of r. Here the Schwarzschild radius R_S is dependent on mass $m(r)$ and radius r. When the equality in Equation (29) is considered, substituting Equation (28) into Equation (28) gives

$$\left[\frac{\rho(R_S)+\frac{p_0}{c^2}\left(\frac{\rho(R_S)}{\rho_0}\right)^{\gamma}}{\gamma\frac{p_0}{\rho_0}\left(\frac{\rho(R_S)}{\rho_0}\right)^{\gamma-1}\left(\frac{d\rho(r)}{dr}\Big|_{r=R_S}\right)}\right]\left[1+8G\pi R_S^2\frac{p_0}{c^4}\left(\frac{\rho(R_S)}{\rho_0}\right)^{\gamma}\right]=0\,, \qquad (30)$$

If only the p-ρ relation like Equation (22) or Equation (26) is used, there is no solution of $\rho(R_S)=0$ to the black hole for $\gamma>=2$, revealed in Equation (30). A reachable situation of $\rho(R_S)=0$ at $r=R_S$ is given for $\gamma<2$. One possibility to fix this situation is to correct the expression of $P(r)$ by adding one or more terms of order n with $n<\gamma$. A simple correction is to add a term of $-kc^2\rho(r)$ where k is a positive constant, and then Equation (30) becomes

$$\left\{\frac{(1-k)\rho(R_S)+\frac{p_0}{c^2}\left(\frac{\rho(R_S)}{\rho_0}\right)^{\gamma}}{\left[\gamma\frac{p_0}{\rho_0}\left(\frac{\rho}{\rho_0}\right)^{\gamma-1}-kc^2\right]\left(\frac{d\rho(r)}{dr}\Big|_{r=R_S}\right)}\right\}\left[1-\frac{8G\pi R_S^2}{c^2}k\rho(R_S)+8G\pi R_S^2\frac{p_0}{c^4}\left(\frac{\rho(R_S)}{\rho_0}\right)^{\gamma}\right]$$
$$=0, \qquad (31)$$

and, mathematically speaking, it gives a few possible solutions including one at $\rho(R_S)=0$. Then the m-ρ relation becomes

$$m(r)=\left\{\frac{\left[(1-k)\rho(r)+\frac{p_0}{c^2}\left(\frac{\rho(r)}{\rho_0}\right)^{\gamma}\right](4\pi r)}{\left(\gamma\frac{p_0}{\rho_0}\left(\frac{\rho(r)}{\rho_0}\right)^{\gamma-1}-kc^2\right)\left(\frac{d\rho(r)}{dr}\right)}\left[\frac{p_0}{c^2}\left(\frac{\rho(r)}{\rho_0}\right)^{\gamma}-k\rho(r)\right]+\frac{1}{G}\right\}r^2. \qquad (32)$$
$$\frac{2r}{c^2}-\left[\frac{(1-k)\rho(r)+\frac{p_0}{c^2}\left(\frac{\rho(r)}{\rho_0}\right)^{\gamma}}{\left(\gamma\frac{p_0}{\rho_0}\left(\frac{\rho(r)}{\rho_0}\right)^{\gamma-1}-kc^2\right)\left(\frac{d\rho(r)}{dr}\right)}\right]$$

Except for $\rho(r)=0$, the other possible zero solutions in Equation (31) obey

$$\left[1-\frac{8G\pi R_S^2}{c^2}k\rho(R_S)+8G\pi R_S^2\frac{p_0}{c^4}\left(\frac{\rho}{\rho_0}\right)^{\gamma}\right]=0, \qquad (33)$$

or

$$(1-k)\rho(R_S)+\frac{p_0}{c^2}\left(\frac{\rho(R_S)}{\rho_0}\right)^{\gamma}=0 \quad (k>1), \qquad (34)$$

which can give the possibility of $r=R_S$ in Equation (32). In Equation (34), it gives a solution of a Schwarzschild black hole if we can find the mass density such that

$$\rho(R_S)=\left[(k-1)\frac{c^2}{p_0}\right]^{\frac{1}{\gamma-1}}\rho_0^{\frac{\gamma}{\gamma-1}}. \qquad (35)$$

On the other hand, some demonstrations by using Equation (33) are shown in Figure 5 3. One γ case is calculated and shown in Figure 3, where the central density ρ_c is between $2\text{x}10^{18}$ and $1.1\text{x}10^{19}$ kg/m^3. When $m(r)$ in Equation (28) is applied, it is easy to do by changing the value of γ. In this γ case,

Preprints.org (www.preprints.org) | NOT PEER-REVIEWED | Posted: 12 July 2024 doi:10.20944/preprints202109.0354.v2

γ=2.80 in Figure 3. The green line represents the star's radius where r=R_S. Since Equation (18) or (27) describes a non-rotating and uncharged star, r=R_S is the limit of possible solutions due to the denominator. Figure 3 exhibits ρ_c=8x10^{19} kg/m^3 corresponding to the most left curve and ρ_c=1.1x10^{19} kg/m^3 to the most right one so that the radius of the black hole at ρ_c=8x10^{19} kg/m^3 is smaller than that at ρ_c=1.1x10^{19} kg/m^3. In our calculations, the ratio of the star's radius to R_S is 1.14365 at ρ_c=1.1x10^{19} kg/m^3 and 1.12547 at ρ_c=8x10^{19} kg/m^3. In all our calculations, the ratio is convergent to 1.125 as the previous report [39].

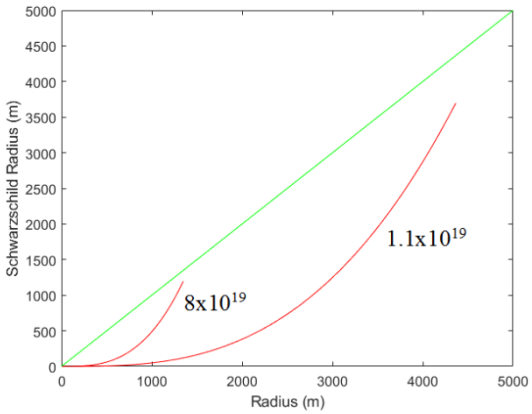

Figure 3. The calculations of the Schwarzschild radius R_S at different radii r according to the TOV equation where ρ_c is 1.1x10^{19} and 8x10^{19} kg/m^3, respectively. The green line represents the black-hole criterion where the star's radius r=R_S. The r-R_S relation for the case of p_0=10$^{32.7}$ dyne/cm^2, ρ_0=ρ_s/2.7=10^{14} g/cm^3, and γ=2.8.

3.4. Proposing Possible Blacks Hole With Finite-Size Nuclear Structures

When considering the charged effect, the exterior spacetime of a charged star can be described by the Reissner-Nordström metric [38-43,55-59]. The Einstein-Maxwell stress tensor of the isotropic fluid and electromagnetic field in terms of the Faraday–Maxwell tensor $F_{\mu\nu}$=$\partial_\mu A_\nu$−$\partial_\nu A_\mu$ is [39,41,42,55,56,58,59]

$$T_\nu^\mu = (P + \rho c^2)u^\mu u_\nu + P\delta_\nu^\mu + \frac{1}{4\pi}\left(F^{\mu\alpha}F_{\alpha\nu} - \frac{1}{4}\delta_\nu^\mu F^{\alpha\beta}F_{\alpha\beta}\right), \qquad (36)$$

where A_μ is an electromagnetic four potential, u^μ is the contravariant four-velocity of the fluid, ρc^2 is the energy density of the fluid, and P is the isotropic pressure in the fluid. Consider the electric charge density ρ_e in the matter then the total charge is [40-43,55,56]

$$Q(r) = r^2E(r)\int_0^r 4\pi r'^2\rho_e(r')\left[1 - \frac{2Gm(r')}{c^2r'} + \frac{KGQ^2(r')}{c^4r'^2}\right]^{-1/2} dr'. \qquad (37)$$

The above gravitational mass $m(r)$ inside the sphere of radius r represents the energy conservation as measured in the star's frame. One can find that another of Einstein's equations gives a differential equation for $m(r)$, [38,39,55,58,59]

$$\frac{dm(r)}{dr} = 4\pi\rho(r)r^2 + \frac{KQ(r)}{c^2r}\frac{dQ(r)}{dr}. \qquad (38)$$

Since $m(r)$ represents the gravitational mass inside the sphere of a radius r, then Equation (38) represents the energy conservation measured in the star's frame [39]. From the covariant conservation of the mass-energy stress tensor, $T_\nu{}^\mu{}_{;\mu}$=0, one gets the hydrostatic equilibrium equation that determines the global structure of electrically charged stars. Then we obtain the modified TOV equation as [39,41-43,55,58,59]

 doi:10.20944/preprints202109.0354.v2

$$\frac{dP(r)}{dr}=-\frac{2G}{r^2}\left(\rho(r)+\frac{P(r)}{c^2}\right)\frac{\left[m(r)+\frac{4\pi r^3}{c^2}\left(P(r)-\frac{KQ^2(r)}{4\pi c^2 r^4}\right)\right]}{\left[1-\frac{2Gm(r)}{c^2 r}+\frac{KGQ^2(r)}{c^4 r^2}\right]}+\frac{KQ(r)}{4\pi r^4}\frac{dQ(r)}{dr}. \quad (39)$$

Furthermore, if an incompressible fluid is considered, then $\rho(r)$ is a constant whole of the body. Therefore, the energy density is also constant in the whole star. Based on this, the small electric-charge effect on mass is discussed next. As mentioned before, the zero-charge case in the Reissner–Nordström metric corresponds to the interior Schwarzschild structure. When a few electric charges exist in the star, the mass distribution is perturbed according to Equation (38). Then the charge $Q(r)$ is treated as a small perturbation, and mass and charge are the forms [39]

$$Q(r)=Q_1(r) \quad (40)$$

and

$$m(r)=m_0(r)+m_1(r), \quad (41)$$

where $m_0(r)$ is the mass of the uncharged star, and $Q_1(r)$ and $m_1(r)$ are the perturbed small charge and mass distributions to be determined. Equation (41) reveals that the total mass in the electric-charge case is more than the uncharged case. Thus, the increasing mass can improve the optimized ratio of r to R_S when a few electric charges are in the neutron star. Next, defining a characteristic length R_c by [39]

$$R_c^2=\frac{3c^2}{8\pi G\rho}, \quad (42)$$

then the r-dependent mass within the sphere of a radius r is

$$m_0(r)=\frac{c^2r^3}{2GR_c^2}=\frac{c^2R_c}{2G}\left(\frac{r}{R_c}\right)^3=\frac{c^2R_c}{2G}x^3, \quad (43)$$

where a dimensionless variable $x=r/R_c$ is introduced. It has been proved that the so-called Schwarzschild limit in an uncharged and non-rotating star gives [39]

$$\frac{c^2R}{GM}=\frac{2R}{R_S}=\frac{9}{4}, \quad (44)$$

which is the same as the limit of our simulations that R/R_S=1.125. Even more, the similar upper-ratio limit for the charged and non-rotating star has been given by [60,61]

$$\frac{R_S}{2R}\le\left[\frac{2R^2+3\left(\frac{KGq^2}{c^4}\right)}{9R^2}+\frac{2}{9R}\sqrt{R^2+3\left(\frac{KGQ(R)^2}{c^4}\right)}\right], \quad (45)$$

where $Q(R)$ is the total charge of the star. Suppose the electric charge density is proportional to the energy density in the smally charged effect, that is,

$$\rho_e=\alpha\sqrt{\frac{G}{K}}\rho, \quad (46)$$

where α is a proportional constant. Then the electric-charge distribution is given by [39]

$$Q_1(x)=\frac{3}{4}\alpha\left(\sin^{-1}x-x\sqrt{1-x^2}\right), \quad (47)$$

and the mass distribution is [39]

$$m_1(x)=\frac{3}{8}\alpha^2\left(3x-x^3-3\sqrt{1-x^2}\sin^{-1}x\right), \quad (48)$$

 doi:10.20944/preprints202109.0354.v2

if K=G=c=1 is used for natural units. Finally, Equation (44) becomes

$$\frac{Rc^2}{GM} = \frac{9}{4} - 1.529\alpha^2. \quad (49)$$

In Equation (49), it seems that α=0.4044 gives the value at the right side equal to 2.00 but is out of the small-charge range. Actually, it has been pointed out that this quasiblack hole configuration is given by the extremal charged case where α is as high as 0.99 [38]. On the other hand, a smaller value has been reported for a similar case, a charged perfect fluid model with high compactness [62]. In this model, the minimum value in Equation (45) gives

$$\frac{1}{u_{max}} = \frac{c^2 R_{min}}{GM} = \frac{2R_{min}}{R_S} = \frac{1}{0.5337972212} = 1.87337 < 2, \quad (50)$$

which the radius of the compact star is smaller than the Schwarzschild radius. In this minimum condition, the total charge is $Q(R_{min}) = 1.648824 \times 10^{20}\ C$ and the one corresponding event horizon is

$$r_+ = \frac{GM}{c^2} + \sqrt{\frac{G^2M^2}{c^4} - \frac{KGQ(R_{min})^2}{c^4}} \approx 1.194\frac{GM}{c^2} = 0.597R_S, \quad (51)$$

where $M = M_\odot$. In this reported case, $r_+ < R_{min} < R_S$. According to this, a double-characteristic structure, based on the perfect fluids, is proposed to explain the existence of the black hole as shown in Figure 4. This kind of black hole has a total charge zero or nonzero, and may have three regions or more. In this structure, the inner region denoted by I is a positively charged region and the almost whole mass of the black hole exists here, the middle region denoted by II is a neutrally thin region to protect the inside positive charges from easily electrically neutralizing the outside negative charges, and the outmost region denoted by III is a very thin negatively charged layer to balance the inner positive charges. One possible constitution in Region I is protons, which are covered by the neutral Region II consisting of materials such as neutrons. The appropriate metric used in Region I and Region II is the Reissner–Nordström metric. Kerr–Newman metric where Region I and Region II have no rotation. If the rotation is small so that the R_Q [62] is a good approximation, then the Kerr-Newman metric can be used here. On the other hand, the appropriate metric outside Region III can be the Kerr-Newman metric because all charges enclosed by the outer dashed circle are zero or nonzero, and the total angular momentum is also zero or nonzero. Therefore, the charged term $R_{Q,new}$ and rotation term a_{new} are both zero or nonzero dependent on the characteristics of Region III. The whole negative charges in Region III are supposed to move in circular orbitals and produce zero electric fields in Region I and Region II. Because the minimum radius is $R_{min} = 0.9367R_S$ for the case of the total charge $Q = 1.648824 \times 10^{20}\ C$ [62], this negatively charged region can exist between R_{min} and R_S to ensure that the whole structure is within the Schwarzschild radius R_S. The amount of negative charges may be different from Q to reach the criterion of a black hole. In such a case, the balanced total charge in Region III also changes. The most advantaged composition of Region III to form a black hole is the electron because its mass is only about 9.1 x10^{-31} kg. However, there is a very strong Coulomb attraction between Region I and Region III. If Region III is initially at rest, it will be quickly attracted toward Region II and Region I. Therefore, one possible situation for Region III consisting of electrons is to move ultra-relativistically around Region I and Region II a little similar to the M87 black hole image surrounded by a hot disk accretion [16]. The equatorial motions of charged test particles in the Kerr-Newman metric have been studied [63-67], in which the case of l = 0 in the Kerr-Newman-Taub-NUT metric is also our research here. Based on these report [63-67], our model can have strongly support.

Preprints.org (www.preprints.org) | NOT PEER-REVIEWED | Posted: 12 July 2024 doi:10.20944/preprints202109.0354.v2

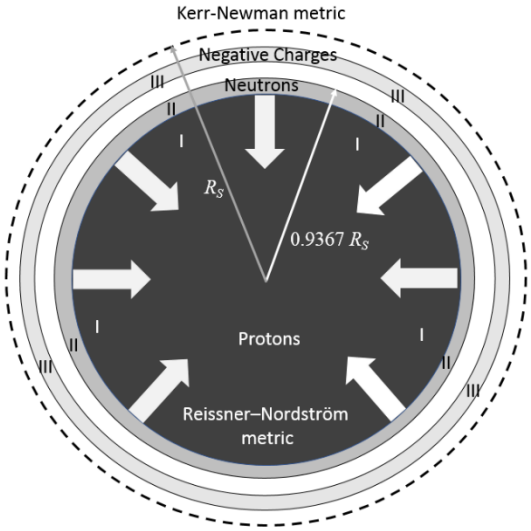

Figure 4. The cross-section structure of a double-characteristic black hole with a total charge zero or nonzero. This kind of black hole has a positively charged region I, possibly consisting of protons, which is covered by neutral thin Region II such as neutrons. Their outmost thin layer consists of negative charges denoted by Region III. These negative charges such as electrons may move corotating or counter-rotating surrounding Region I and Region II. The place including Region I and Region II is described by the Reissner–Nordström metric and the place in Region III and outside this Region is described by the Kerr–Newman metric. Region III exists between $0.9367R_S$ and R_S in which the minimum radius $R_{\min}$=$0.9367R_S$ of Region II and total charge $Q = 1.648824 \times 10^{20}\ C$ in Region I are considered [62]. Due to this structure of the black hole, the radius of Region III is required to be less than the outer event horizon $r_+ = \left(R_S + \sqrt{R_S^2 - 4a_{new}^2 - 4R_{Q,new}^2}\right)/2$, then the criterion of a Kerr-Newman black hole. Therefore, a finite-size structure [38,39,62] in the Reissner–Nordström metric transforms into a black hole described by the Kerr–Newman metric.

Then we start from the Kerr-Newman metric to discuss this model mentioned above. This starting point is chosen by the reason that Region III includes rotating charges, so it is better to describe the spacetime by the Kerr-Newman metric than the Reissner–Nordström metric which is only suitable for Region I and Region II. The Kerr-Newman metric is [25,44,68]

$$ds^2 = \frac{\Delta - a^2\sin^2\theta}{\rho^2}c^2dt^2 - \frac{\rho^2}{\Delta}dr^2 - \rho^2 d\theta^2 + 2ac\sin^2\theta\left(1 - \frac{\Delta - a^2\sin^2\theta}{\rho^2}\right)dtd\phi - \left[\rho^2 + a^2\sin^2\theta\left(2 - \frac{\Delta - a^2\sin^2\theta}{\rho^2}\right)\right]\sin^2\theta d\phi^2, \quad (52)$$

where

$$\rho^2 = r^2 + a^2\cos^2\theta, \quad (53)$$

$$\Delta = r^2 - rR_S + a^2 + R_Q^2, \quad (54)$$

and

$$R_Q^2 = \frac{KGQ^2}{c^4}. \quad (55)$$

The term related to angular momentum is $a = J/Mc$. Three conservation constants of motions for a test particle of mass m and electric charge q can be obtained by Hamiltonian [65,66], which are

$$g_{\mu\nu}dx^\mu dx^\nu = -m^2c^2, \quad (56)$$

$$E = -\pi_t = -g_{tt}\dot{t} - g_{t\phi}\dot{\phi} + qA_t, \quad (57)$$

 doi:10.20944/preprints202109.0354.v2

and

$$L = \pi_\phi = g_{\phi t}\dot{t} + g_{\phi\phi}\dot{\phi} - eA_\phi, \tag{58}$$

where the vector potential for electromagnetic fields is [65-67,69]

$$A = A_\mu dx^\mu = \frac{Qr}{\rho^2}(dt - a\sin^2\theta d\phi). \tag{59}$$

The equation of motion is

$$m\frac{Du^\mu}{D\tau} = eF^\mu_\nu u^\nu, \tag{60}$$

where $F^\mu_\nu = \partial_\nu A^\mu - \partial_\mu A^\nu$. Using the general form of the Hamilton-Jacobi equation, the following differential equations governing the motion of the charged test particle can be deduced [63-67,70]:

$$\rho^2\frac{dr}{d\lambda} = \pm P_R(r)^{1/2}, \tag{61}$$

$$\rho^2\frac{d\theta}{d\lambda} = \pm V^{1/2}, \tag{62}$$

$$\rho^2\frac{d\phi}{d\lambda} = -\frac{(aE\sin^2\theta - cL)}{\sin^2\theta} + \frac{a[E(r^2+a^2) - acL + KqQr]}{\Delta}, \tag{63}$$

and

$$\rho^2\frac{dt}{d\lambda} = (r^2+a^2)[E(r^2+a^2) - acL + KqQr] - (a^2E\sin^2\theta - acL), \tag{64}$$

where λ is the affine parameter related to the proper time τ of the particle divided by its mass m [63,67,70,71], the Carter constant is zero here [63-65,70],

$$P_R(r) = [E(r^2+a^2) - acL - KqQr]^2 - \Delta[m^2c^4r^2 + (cL - aE)^2], \tag{65}$$

and

$$V = [(cL - aE)^2 - m^2c^4a^2\sin^2\theta] - \left(\frac{aE\sin^2\theta - cL}{\sin\theta}\right)^2. \tag{66}$$

We consider the circular orbits in Figure 4, where the satisfied conditions are

$$P_R(r) = 0 \tag{67}$$

and

$$\frac{dP_R(r)}{dr} = 0. \tag{68}$$

Three orbital configurations have been discussed at $\theta = 0, \pi$, $\theta = \pi/2$, and $\theta = \pm\sqrt{\bar{K}/\bar{a}^2}$, where $\bar{K}$ and $\bar{a}$ are defined in the reference [65]. From the latitudinal equation of motion, it follows that the circular orbit passing through $\theta = 0$ and π only exists when Q=0 [63,64]. Therefore, in our case of $Q \neq 0$, we simply consider the circular motion in the equatorial plane. In the case of particles with nonzero mass and a high specific charge, the above two conditions for the circular orbitals give two solutions for E and L, which are [64,65]

 doi:10.20944/preprints202109.0354.v2

$$E_{\pm}=\left(-\frac{KqQ}{r}\right)\frac{R_S r-2a^2-2R_Q^2\pm 2a\sqrt{r^2-R_S r+a^2+R_Q^2}}{2r^2-3R_S r+4a^2+4R_Q^2\pm 4a\sqrt{r^2-R_S r+a^2+R_Q^2}} \quad (69)$$

and

$$L_{\pm}=\left(-\frac{KqQ}{cr}\right)\frac{a\left(R_S r-2a^2-2R_Q^2\right)\pm 2(r^2-a^2)\sqrt{r^2-R_S r+a^2+R_Q^2}}{2r^2-3R_S r+4a^2+4R_Q^2\pm 4a\sqrt{r^2-R_S r+a^2+R_Q^2}}. \quad (70)$$

If the rotation of the charged test particle on the equatorial plane is counter-rotating, then the energy and angular momentum of the charged test particle are calculated with the sign '-' in the above two equations. Otherwise, the sign '+' is chosen if the charged test particle moves corotating. In this metric, the frame-dragging effect is

$$\Omega=\frac{u^{\phi}}{u^{t}}=-\frac{g_{\phi t}}{g_{tt}}. \quad (71)$$

Although it exists in the Kerr-Newman source, the circular orbital can be corotating (prograde) and counter-rotating (retrograde) in the locally nonrotating frame [64,65,67,71]. Then we can calculate the energy E and L by using the known a and R_Q. According to Ref. 62 [62], the total charge $Q=1.648824\times10^{20}\ C$ gives

$$R_Q=\sqrt{\frac{KGQ^2}{c^4}}=0.48R_S. \quad (72)$$

In our model, we consider electrons moving in circular orbitals on the equatorial plane, surrounding Region I and Region II at radius r between $0.9367R_S$ and R_S, where Region I and Region II are static, so the rotation term is a=0 and the charged term is R_Q=$0.48R_S$ in the E and L calculations. The spacetime in Region I and Region II is described by the Reissner–Nordström metric. Because the negative charges in Region III move ultra-relativistically surrounding Region I and Region II, the spacetime in and outside Region III is described by the Kerr-Newman metric. Therefore, the nonzero new rotation term a_{new} exists which is produced by the surrounding negative charges. A simple choice of the negative charge in Region III is the electron whose mass is very tiny and only 9.1×10^{-31} kg, so we consider electrons as the negative charges in Region III.

Next, we discuss how to construct a finite-size structure to satisfy the criterion of a Kerr-Newman black hole. The event horizons of the Kerr-Newman black hole, determined by Δ=0, are

$$r_{\pm}=\frac{R_S\pm\sqrt{R_S^2-4a_{new}^2-4R_{Q,new}^2}}{2}, \quad (73)$$

where r_- is the inner event horizon and r_+ is the outer horizon event. If the Kerr-Newman black hole is expected, then it needs $r_+\geq R_{min}=0.9367R_S$ at least. In order to reach this criterion, small and small a_{new} and $R_{Q,new}$ are better. Based on this, we use negative charges in Region III to balance the positive charges in Region I so the term $R_{Q,new}$ can be reduced to zero. However, due to the surrounding electrons, the nonzero angular momentum of electrons brings nonzero a_{new}. For the purpose of decreasing the new rotation term a_{new}, both corotating and counter-rotating electrons are considered. The simple situation is that the corotating and counter-rotating electrons are equal, and their total charges are -Q, $-1.648824\times10^{20}\ C$. When the rotation term a of Region I and Region II is zero, the angular momenta of the corotating and counter-rotating electrons are the same in magnitude, which are

 doi:10.20944/preprints202109.0354.v2

$$L_{\pm}(a=0)=\pm\left(-\frac{KqQ}{cr}\right)\frac{2r^2\sqrt{r^2-R_Sr+R_Q^2}}{2r^2-3R_Sr+4R_Q^2}. \quad (74)$$

Therefore, if these two kinds of electrons are equal in number and move in opposite directions at very close orbitals, then the summation of their angular momenta is ~ 0. In the simple situation, we have a_{new}~0 and $R_{Q,new}$~0, so

$$r_+=\frac{R_S+\sqrt{R_S^2-4a_{new}^2-4R_{Q,new}^2}}{2}\cong R_S>0.9367R_S. \quad (75)$$

In this case, the event horizon is larger than the radius of Region III and includes Region I and Region II. The number of total electrons is N=1.029x10^{39}. As a result, a Kerr-Newman black hole with a_{new}=0 and $R_{Q,new}$=0, or a Schwarzschild black hole is formed by using our model in Figure 4. In such a case, the radii of the counter-rotating and corotating electrons are denoted by r_1 and r_2, respectively. The radii satisfying r_+>=max(r_1,r_2) are drawn in Figure 5(a), where the red points are the allowed radii for the whole structure including Region I, Region II, and Region III which can be black holes. More allowed radii are close to R_{min}=0.9367R_S, and the allowed radii decrease when they are close to R_S. On the other hand, the corresponding orbital energy and angular momentum for the counter-rotating (red) and corotating (green) electrons are plotted in Figure 5(b) and 5(c), where the very small rotation term $a\leqq 0.03R_S$ is considered with a constant R_Q=0.48R_S, and the radii are between 0.938R_S and 1.007R_S. Because the surrounding electrons are attracted by the positive charges, the orbital energy is negative no matter if it is a counter-rotating or corotating electron. Both kinds of electrons have the same energy when a=0. In Figure 5(c), the angular momenta show the counter-rotating electron has positive angular momentum and the corotating electron has negative angular momentum by definition. When a=0, both kinds of electrons have the same angular momenta in magnitude.

Not only the Schwarzschild black hole but also the Kerr-Newman black hole can be formed in our model. Next, we consider the occupation of the counter-rotating electrons is $\alpha_1 N$ and the occupation of the corotating electrons is $\alpha_2 N$, where $\alpha_1\geqq 0$ and $\alpha_2\geqq 0$, and $\alpha_1+\alpha_2$ is not necessarily equal to one. If $\alpha_1+\alpha_2<1$. The finite-size structure including Region I, Region II, and Region III is positively charged. Otherwise, If $\alpha_1+\alpha_2>1$, the finite-size structure is negatively charged. Therefore, if $\alpha_1+\alpha_2\neq 1$, we have nonzero total charge $Q_{new}=(1-\alpha_1-\alpha_2)Q$ and

$$R_{Q,new}^2=\frac{KG(1-\alpha_1-\alpha_2)^2Q^2}{c^4}=(1-\alpha_1-\alpha_2)^2R_Q^2. \quad (76)$$

If L_1 is the angular momentum of the counter-rotating electron and L_2 is the angular momentum of the corotating electron, then the total angular momenta are

$$L=\alpha_1 NL_1+\alpha_2 NL_2, \quad (77)$$

and the new corresponding rotation term of the finite-size structure is

$$a_{new}=\frac{L}{[M+(\alpha_1+\alpha_2)Nm_e]c}\cong\frac{L}{M_\odot c}. \quad (78)$$

In order to have a small a_{new}, the values of α_1 and α_2 are expected to be close to each other. Some allowed radii of the counter-rotating and corotating electrons are plotted in Figure 5(d), where α_1 is fixed at 0.50 and four different α_2 values, 0.28 (purple), 0.34 (cyan), 0.45 (green), and 0.62 (yellow) are chosen. As α_2 increases, the trend of the allowed r_2 decreases at the same r_1. In this case of α_1=0.50, the minimum α_2 is 0.277 by our calculations. In conclusion, our model can construct black hole and the property of the black hole is dominated by the corotating and counter-rotating electrons, which makes the black hole charged or uncharged, and rotating or non-rotating.

Preprints.org (www.preprints.org) | NOT PEER-REVIEWED | Posted: 12 July 2024 doi:10.20944/preprints202109.0354.v2

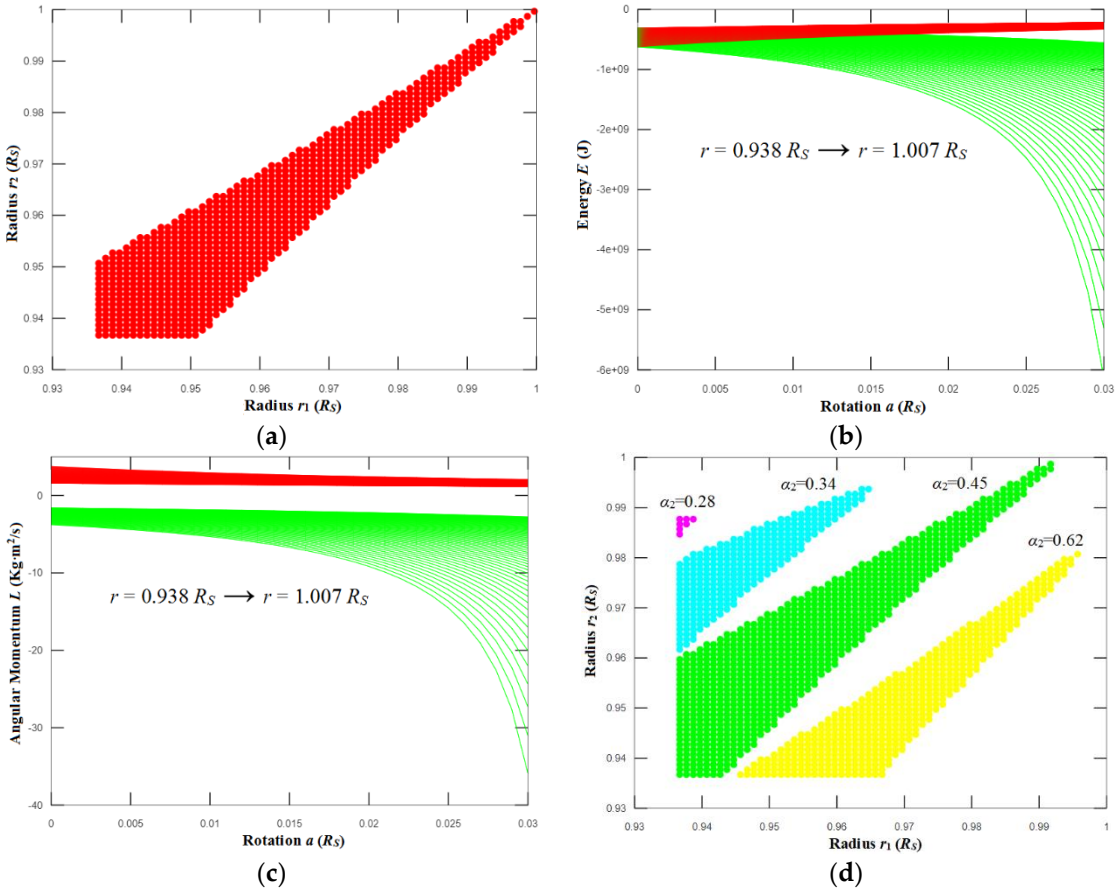

Figure 5. (a) When α_1=α_2=0.5, the radii of the counter-rotating and corotating electrons denoted by r_1 and r_2, respectively, satisfy r_+>=max(r_1,r_2) here. (b) The corresponding orbital energy for the counter-rotating (red) and corotating (green) electrons where the very small rotation term $a \leqq 0.03R_S$ is considered with a constant R_Q=0.48R_S, and the radii are between 0.938R_S and 1.007R_S, where both are plotted from up to down. (c) the corresponding angular momentum for the counter-rotating (red) and corotating (green) electrons are plotted in Figure 5(b) and 5(c), where the very small rotation term $a \leqq 0.03R_S$ is considered with a constant R_Q=0.48R_S, and the radii are between 0.938R_S and 1.007R_S, where the red parts are plotted from down to up and the green parts are plotted form up to down. (d) When α_1 = 0.5 and four α_2 values, 0.28 (purple), 0.34 (cyan), 0.45 (green), and 0.62 (yellow) are chosen, the allowed radii r_1 and r_2 satisfying r_+>=max(r_1,r_2) are plotted. As α_2 increases, the trend of the allowed r_2 decreases at the same r_1.

Furthermore, the Schwarzschild radius is linearly proportional to $m(R_S)$=M so the average density of a black hole is

$$\bar{\rho} = \frac{3c^6}{32\pi G^3 M^2}. \tag{79}$$

It shows that the average density is inversely proportional to the total mass square. Therefore, the higher the average density is, the lower the total mass and radius.

3.5. Energy Conservation Between Different Energy Transformations

In the following, we consider the possible size of a neutron star. Due to the supernova producing ultra-high pressure, 2N neutrons theoretically produce. Because of the supernova, in fact, αN neutrons transfer to the radiation energy and the work to compress the materials, and (2-α)N neutrons are left there. The volume is changed from V_0 to V. Then the total kinetic energy of the rest (2-α)N neutrons within the volume V in the ultra-relativistic condition is [46]

 doi:10.20944/preprints202109.0354.v2

$$U_N \approx \frac{2\pi V m_n^4 c^5}{h^3}\left(\frac{p_f}{m_n c}\right)^4 = \frac{2\pi V c p_f^4}{h^3} = \frac{3(2-\alpha)Nhc}{4}\left[\frac{3(2-\alpha)N}{8\pi V}\right]^{1/3}, \quad (80)$$

where the momentum of Fermi energy for the neutron gas is

$$p_f = h\left[\frac{3(2-\alpha)N}{8\pi V}\right]^{1/3}. \quad (81)$$

Finally, the total energy of these (1-α)N and (2-α)N neutrons approximates to

$$U_{total}^{rest} \approx U_N + (1-\alpha)Nm_e c^2 + (2-\alpha)Nm_n c^2 + U_g^{rest}$$

$$\approx \frac{3(2-\alpha)Nhc}{4}\left[\frac{3(2-\alpha)N}{8\pi V}\right]^{1/3} + (1-\alpha)Nm_e c^2 + (2-\alpha)Nm_n c^2 + U_g^{rest}, \quad (82)$$

where the self-energy of gravity forming those (2-α)N neutrons in the homogeneous density distribution is

$$U_g^{rest} = \frac{3G(2-\alpha)^2 m_n^2 N^2}{5}\left(\frac{4\pi}{3V}\right)^{1/3}. \quad (83)$$

Similarly, when we consider the inhomogeneous case, then the rest self-energy of gravity of the star with a radius of R' is

$$U_g^{rest} = \int_0^{R'} 4\pi c^2 \rho(r)\frac{\left[1-e^{-\lambda(r)}\right]}{2}dr = \int_0^{R'} \frac{G4\pi r^2 \rho(r)dr}{r}\int_0^r 4\pi r'^2 \rho(r')dr', \quad (84)$$

where $R'<R$ and $e^{-\lambda(r)}$ is the metric potential in Equation (1). Considering energy conservation, it gives

$$U_{total}^{rest} < \frac{3(2N)hc}{4}\left[\frac{3(2N)}{8\pi V_0}\right]^{1/3} + Nm_e c^2 + 2Nm_n c^2 + U_g < \infty. \quad (85)$$

From Equation (85), it clearly shows that $V>0$ and $V<V_0$ so the (2-α)N neutrons form a finite-size volume, and they cannot shrink to a point.

3.6. The Up Limit of The Nuclear Size In The Black Hole

In fact, it has been revealed that the upper-mass limit of the white dwarf star, calculated by the homogeneous-density model, is close to the inhomogeneous-density model by considering dp/dr and dm/dr [45,46]. The correction is to multiply the self-energy in the homogeneous-density model by a constant of 1.124 [45,46]. in such a compact star, the homogeneous-density model is a good approximation. Therefore, we can adopt the homogeneous density in both Equations (16) and (84) for the compact star. Furthermore, by ignoring the total energy of rest electrons, Equation (85) gives

$$\alpha N m_n c^2 + \left[2(2)^{1/3} - (2-\alpha)(2-\alpha)^{1/3}\left(\frac{1}{\beta}\right)^{1/3}\right]\frac{3Nhc}{4}\left(\frac{3N}{8\pi V_0}\right)^{1/3} + \frac{3Gm_n^2 N^2}{5}\left[4-(2-\alpha)^2\left(\frac{1}{\beta}\right)^{1/3}\right]\left(\frac{4\pi}{3V_0}\right)^{1/3} > 0, \quad (86)$$

where $V=\beta V_0$ with $0<\beta<1$. When α is small and considering the Taylor expansion to the linear term for $(2-\alpha)^{1/3}$, then Equation (86) becomes

$$\alpha N m_n c^2 + 2(2)^{1/3}\left[1-\left(1-\frac{\alpha}{2}\right)\left(1-\frac{\alpha}{6}\right)\left(\frac{1}{\beta}\right)^{1/3}\right]\frac{3Nhc}{4}\left(\frac{3N}{8\pi V_0}\right)^{1/3} + \frac{3Gm_n^2 N^2}{5}\left[4-(4-4\alpha+\alpha^2)\left(\frac{1}{\beta}\right)^{1/3}\right]\left(\frac{4\pi}{3V_0}\right)^{1/3} > 0. \quad (87)$$

 doi:10.20944/preprints202109.0354.v2

After arranging the above equation, it gives

$$\alpha m_n c^2 (\beta)^{1/3} + 2\left[(\beta)^{1/3} - 1 + \frac{2}{3}\alpha - \frac{1}{12}\alpha^2\right]\frac{3hc}{4}\left(\frac{3N}{4\pi V_0}\right)^{1/3} + \frac{3}{5}Gm_n^2 N\left[4(\beta)^{1/3} - (4 - 4\alpha + \alpha^2)\right]\left(\frac{4\pi}{3V_0}\right)^{1/3} > 0. \quad (88)$$

Then solving α, the range is

$$\max\left\{0, \frac{\left\{-(square\ root\ term) + \left[m_n c^2 (\beta V_0)^{1/3} + hc\left(\frac{3N}{4\pi}\right)^{1/3} + \frac{12}{5}Gm_n^2 N\left(\frac{4\pi}{3}\right)^{1/3}\right]\right\}}{\left[\frac{hc}{4}\left(\frac{3N}{4\pi}\right)^{1/3} + \frac{6}{5}Gm_n^2 N\left(\frac{4\pi}{3}\right)^{1/3}\right]}\right\} < \alpha$$

$$< \min\left\{2, \frac{\left\{(square\ root\ term) + \left[m_n c^2 (\beta V_0)^{1/3} + hc\left(\frac{3N}{4\pi}\right)^{1/3} + \frac{12}{5}Gm_n^2 N\left(\frac{4\pi}{3}\right)^{1/3}\right]\right\}}{\left[\frac{hc}{4}\left(\frac{3N}{4\pi}\right)^{1/3} + \frac{6}{5}Gm_n^2 N\left(\frac{4\pi}{3}\right)^{1/3}\right]}\right\}, \quad (89)$$

where the square root term is

$$square\ root\ term = \left\{\left[m_n c^2 (\beta V_0)^{1/3} + hc\left(\frac{3N}{4\pi}\right)^{1/3} + \frac{12}{5}Gm_n^2 N\left(\frac{4\pi}{3}\right)^{1/3}\right]^2 - 4\left[\frac{hc}{8}\left(\frac{3N}{4\pi}\right)^{1/3} + \frac{3}{5}Gm_n^2 N\left(\frac{4\pi}{3}\right)^{1/3}\right]\left[\frac{3hc}{2}\left(\frac{3N}{4\pi}\right)^{1/3} + \frac{12}{5}Gm_n^2 N\left(\frac{4\pi}{3}\right)^{2/3}\right]\left[1 - (\beta)^{1/3}\right]\right\}^{1/2}. \quad (90)$$

This square root term depends on N, β, and V_0. All other parameters are well-known constants. This α range approximately gives the exhaust of neutron particles in the event of a supernova. Equation (89) can estimate the mass of a black hole and its nuclear volume [20] by considering the number of neutrons in the original star.

Then according to Equation (90), we demonstrate two situations and theoretically study the trend between the low limit α and β as shown in Figure 5. The first situation is the star radius r equal to $R_\odot$, in which three cases of $2M_\odot$, $3M_\odot$, and $4M_\odot$ are considered in this situation. In our calculations, three curves for the three cases of the first situation are plotted in Figure 5, and they are indigo ($2M_\odot$), green ($3M_\odot$), and red ($4M_\odot$) curves from the left to the right. These three cases are also circled and denoted by r=$R_\odot$. The other three cases for the second situation circled and denoted by r=0.1 $R_\odot$ in Figure 5, are the indigo, green, and red curves corresponding to $2M_\odot$, $3M_\odot$, and $4M_\odot$ from the left to the right. The radius of each star in the first situation is 10 times larger than that of each star in the second situation. Therefore, in the second situation, the density of the star is 1,000 times larger than that of the star with the same mass in the first situation. In both situations, the curves of the lightest star ($2M_\odot$) are at the most left and the curves of the heaviest star ($4M_\odot$) are at the most right. In these

 doi:10.20944/preprints202109.0354.v2

curves, the low-limit α means the minimum exhausting energy and β represents the ratio of the final volume to the initial volume for each star experiencing supernova. If a smaller final volume is expected after a supernova, the exhausting energy has to be more than that of the larger final volume because a lot of exhausting energy is used to do work on compressing the initial volume to a smaller final one. In Figure 5, the low-limit α increases from 10% to 90% when β decreases from about 10^{-13} to 10^{-19} for the 4-$M_\odot$ case of the first situation, and from about 10^{-10} to 10^{-16} for the same case of the second situation. Theoretically speaking, the denser star needs more energy to compress itself to a smaller volume than a less dense star. For example, exhausting 10% mass or considering the low limit α= 0.2 can reach a much smaller β of about 10^{-13} in the first situation than it in the second situation, where β is about 10^{-10}, a much higher value. All these results are obtained by considering energy conservation.

Recently, the similarity between the neutron star and the black hole has been discussed [47]. The compression of neutrons and helium atoms under extreme pressure has been studied [72,73]. Neutrons and protons are both baryons composed of quarks and gluons. They have much ability to change their sizes and the force inside them is the strong interaction which is 10^{39} times larger than gravity. The experiment about the distribution of pressure inside the proton also showed the average peak pressure about of 10^{35} Pascals near the center of a proton [34]. This pressure much exceeds the pressure estimated by most neutron stars. When we compress the rest (2-α)N neutrons, they can become much smaller as shown in the quark-matter phase diagrams [74,75] and all the volume V is within the event horizon of a black hole. In our discussions, we want to reveal the truth that the so-called curvature singularity inside the black hole, such as r=0 in the Schwarzschild black hole, is a mathematical discussion in the Schwarzschild metric, not from physical foundation. In the traditional black-hole theory, the knowledge tells us that everything inside the black hole inevitably reaches r=0 due to strong gravity, without considering any physical reality, and energy input and output. The evolution from the star to a black hole should follow energy conservation, and the black hole reasonably has a finite-size nucleus in it, not a singularity.

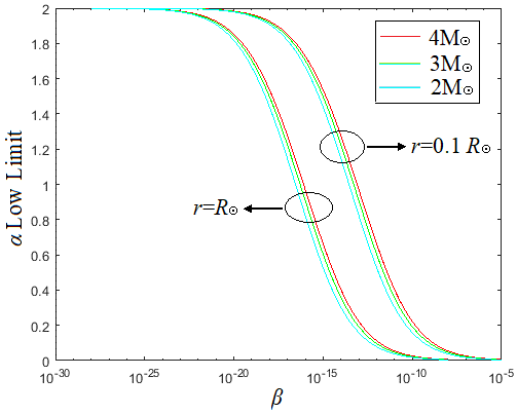

Figure 5. A demonstration between α and β according to Equation (90). There are two groups plotted where the right group is 1,000 denser than the left group. Each group includes three cases where the mass of the star is 2$M_\odot$, 3$M_\odot$, and 4$M_\odot$ from left to right, and the radius of the star is the same in each case. The results show that the denser star wastes more energy to reduce its size at the same final volume.

4. Removing Curvature Singularities Of The Black Hole Through A Finite Nuclear Core In The Schwarzschild-Like And Reissner-Nordstrøm-like Metrics - A Simple Review

The curvature singularity problems have been specially solved in 2005, and the way to cure the pathologies existing in the theory of General Relativity is by using a Gaussian mass density distribution and a Gaussian charge density distribution [21-28] which is the same concept as our thoughts in this paper. No matter the singularity at the origin or on the ring, it can be removed by this method. According to the results [21-28], our finite-size nucleus model can also remove the ring singularity from the theory of General Relativity. We will summarize their works in the Schwarzschild-like and Reissner-Nordstrøm-like metrics as follows.

 doi:10.20944/preprints202109.0354.v2

A popular way to cure the pathologies in the theory of gravity such as the curvature singularities in the black holes is the noncommunity first proposed in 2005 [21]. Noncommunity is an intrinsic property of the manifold without depending on curvature. The physical effect of noncommunity is that the pointlike body is no more meaningful and the smeared body is the only thing that has to be dealt with [21]. In this situation, this concept is realized by substituting pointlike structures with a Gaussian function with minimal width $\sqrt{\vartheta}$ describing the corresponding smeared structures [21]. Then the Gaussian mass density is proposed to be [21-25,27,28]

$$\rho_\vartheta(\vec{r}) = \frac{M}{(4\pi\vartheta)^{3/2}} exp\left(-\frac{\vec{r}^2}{4\vartheta}\right), \tag{91}$$

where M is the total mass of the source and $\vec{r}$ is the position vector. The event horizon radius r_H can be found where $g_{00}(r_H)=0$ so, considering the linearized elements of the Schwarzschild metric, it is determined by the equation

$$r_H = \frac{2GM}{\sqrt{\pi}c^2}\gamma\left(\frac{1}{2};\frac{r_H^2}{4\vartheta}\right), \tag{92}$$

where the incomplete lower Gamma function is defined by [21-26,28]

$$\gamma\left(\frac{b}{a};x\right) = \int_0^x dt t^{b/a-1}e^{-t}. \tag{93}$$

Then the expression of the mass M in terms of r_H is

$$M(r_H) = \frac{\sqrt{\pi}c^2 r_H}{2G\gamma(1/2\,;r_H^2/4\vartheta)}. \tag{94}$$

In the limit of $r_H/\sqrt{\vartheta} \ll 1$, it leads to

$$M \to M_0 = \frac{c^2\sqrt{\pi\vartheta}}{2G}. \tag{95}$$

It implies a minimum nonzero mass to allow the existence of the event horizon in the noncommutative geometry. When $M=M_0$, the event horizon is shrunk to the origin, and the event horizon disappears when $M<M_0$.

When we apply Equation (91) directly on the full Schwarzschild line element, the mass distribution is [22]

$$m(r) = \frac{2M}{\sqrt{\pi}}\gamma\left(\frac{3}{2};\frac{r^2}{4\vartheta}\right). \tag{96}$$

The event horizon radius r_H is determined by the equation [22]

$$r_H = \frac{4GM}{\sqrt{\pi}c^2}\gamma\left(\frac{3}{2};\frac{r_H^2}{4\vartheta}\right). \tag{97}$$

This equation gives one degenerate event horizon at $M=M_0=1.9\sqrt{\vartheta}c^2/G$ [22]. Especially, when $M>M_0$, there are two event horizons much different from the single event horizon of the conventional Schwarzschild metric based on the pointlike source at the center. The other result shows the event horizon when $M<M_0$. This research gives no curvature singularity at the origin in replacing a regular de Sitter core at a short distance [22].

Similar discussions can be extended to the charged black hole where the Gaussian charge distribution is introduced as [23,28]

$$\rho_{el}(\vec{r}) = \frac{Q}{(4\pi\theta)^{3/2}} exp\left(-\frac{\vec{r}^2}{4\vartheta}\right), \tag{98}$$

Preprints.org (www.preprints.org) | NOT PEER-REVIEWED | Posted: 12 July 2024 doi:10.20944/preprints202109.0354.v2

where Q is the total charge. Then the electric field distribution is obtained [23,25,28]

$$E(r) = \frac{KQ}{\sqrt{\pi} r^2} \gamma\left(\frac{3}{2}; \frac{r^2}{4\vartheta}\right), \tag{99}$$

where K is Coulomb's constant. The mass distribution function is the same as Equation (96) in the Schwarzschild-like metric. Finally, the Reissner-Nordstrøm-like metric is obtained as

$$ds^2 = -g_{00} dt^2 + g_{00}^{-1} dr^2 + r^2 d\Omega^2, \tag{100}$$

where

$$g_{00} = 1 - \frac{2Gm(r)}{c^2 r} - \frac{KGQ^2}{c^4 r^2}\left[\gamma^2\left(\frac{1}{2}; \frac{r^2}{4\vartheta}\right) - \frac{r}{\sqrt{2\vartheta}}\gamma\left(\frac{1}{2}; \frac{r^2}{2\vartheta}\right)\right] \tag{101}$$

with

$$m(r) = \frac{2M}{\sqrt{\pi}}\gamma\left(\frac{3}{2}; \frac{r^2}{4\vartheta}\right). \tag{102}$$

When we compare the above solution to the conventional Reissner-Nordstrøm metric at a large distance, it means that the gravitational and electrical contributions are indistinguishable, and the asymptotic observer measures the total mass-energy including both contributions only. Therefore, considering the gravitational energy-momentum tensor $T_\nu^\mu|_{matt}$ and the electromagnetic energy-momentum tensor $T_\nu^\mu|_{el}$, the total mass-energy of the electro-gravitational system is defined as

$$M_{el-g} = \oint_\Sigma d\sigma^\nu \, (T_\nu^0|_{matt} + T_\nu^0|_{el}), \tag{103}$$

where Σ is a t=constant, closed three-dimensional surface at infinity. Then we have [23]

$$g_{00} = 1 - \frac{4GM_{el-g}}{\sqrt{\pi} r c^2}\gamma\left(\frac{3}{2}; \frac{r^2}{4\vartheta}\right) + \frac{KGQ^2}{\pi r^2 c^4}\left[\gamma^2\left(\frac{1}{2}; \frac{r^2}{4\vartheta}\right) - \frac{r\gamma\left(\frac{1}{2}; \frac{r^2}{2\vartheta}\right)}{\sqrt{2\vartheta}} + \sqrt{\frac{2}{\vartheta}} r\gamma\left(\frac{3}{2}; \frac{r^2}{4\vartheta}\right)\right]. \tag{104}$$

It gives the same conventional Reissner-Nordstrøm metric at a large distance. It also results in two event horizons, one event horizon, and no event horizon dependent on the total mass-energy M_{el-g} which is related to r_H and Q. The expression of M is [23]

$$M_{el-g} = \frac{KQ^2}{2\sqrt{2\pi\vartheta} c^2} + \frac{1}{\gamma\left(\frac{1}{2}; \frac{r_H^2}{4\vartheta}\right)}\left\{\frac{\sqrt{\pi}}{4}\frac{r_H c^2}{G} + \frac{KQ^2}{4\sqrt{\pi} c^2 r_H}\left[\gamma^2\left(\frac{1}{2}; \frac{r_H^2}{4\vartheta}\right) - \frac{r_H}{\sqrt{2\vartheta}}\gamma\left(\frac{1}{2}; \frac{r_H^2}{2\vartheta}\right)\right]\right\}. \tag{105}$$

This research also gives the de Sitter spacetime instead of a curvature singularity at a short distance so there is no singularity in the origin neither naked nor shielded by the event horizons [23]. The noncommutative geometry for describing deformations of General Relativity can improve the conventional black hole solutions of Einstein's equation [28]. It cures the singularity behaviors of gravity at the centers of black holes in the above metrics [28].

When we consider the rotating black hole, we can obtain the Kerr-like metric [24]. The Gaussian mass density in Equation (88) is still used here. The total mass M here is

$$M = 4\pi \int_0^\infty dr \, r^2 \rho_\vartheta(r), \tag{106}$$

 doi:10.20944/preprints202109.0354.v2

and the mass distribution function is [28]

$$m(r) = 4\pi \int_0^r dR\, R^2 \rho_\vartheta(R) = \frac{M}{\Gamma\left(\frac{3}{2}\right)} \gamma\left(\frac{3}{2}; \frac{r^2}{4\vartheta}\right). \quad (107)$$

According to the expression of Equation (106), the point r=0 is the origin or the center of the black hole in space, not any point on a ring with a finite radius. As we know, the gravity of the black hole is very strong and it makes all mass together as much as possible. All the mass of a black hole cannot form a ring in space because gravity can make them very close to each other. Therefore, the ring singularity which we consider does not exist in real space. In the following, we use differential geometry to explain it. Usually, the coordinates to describe the Schwarzschild metric are convenient the spherical coordinates (r,θ,Φ) plus the time coordinate t which consists of spacetime with dimension n=4. The difference between the Euclidean spacetime and conventional Schwarzschild spacetime is that the singularity exists at r=0 and a Schwarzschild radius R_S is defined and used. When we discuss the Kerr metric, we can use the Boyer-Lindquist coordinates (r,θ,Φ) and the particular Cartesian coordinates (x,y,z) [11,12]. The Kerr metric in the Boyer-Lindquist is expressed as [15]

$$ds^2 = -c^2 d\tau^2 = \left(\frac{dr^2}{\Delta} + d\theta^2\right)\rho^2 - (cdt - a\sin^2\theta d\phi)^2 \frac{\Delta}{\rho^2} + \left((r^2 + a^2)d\phi - acdt\right)^2 \frac{\sin^2\theta}{\rho^2}, \quad (108)$$

where

$$\rho^2 = r^2 + a^2\cos^2\theta, \quad (109)$$

$$\Delta = r^2 - rR_S + a^2. \quad (110)$$

From Δ=0, the positions of the two event horizons can be solved, which are

$$r_+ = \frac{R_S}{2} + \left[\left(\frac{R_S}{2}\right)^2 - a^2\right]^{1/2}, \quad (111)$$

$$r_- = \frac{R_S}{2} - \left[\left(\frac{R_S}{2}\right)^2 - a^2\right]^{1/2}. \quad (112)$$

Without considering the same time coordinate t, both coordinates can be related to each other as follows

$$x = \sqrt{r^2 + a^2}\sin\theta\cos[(\phi - \arctan(a/r))], \quad (113)$$

$$y = \sqrt{r^2 + a^2}\sin\theta\sin[(\phi - \arctan(a/r))], \quad (114)$$

and

$$z = r\cos\theta. \quad (115)$$

They can form an ellipsoidal surface described by

$$\frac{x^2 + y^2}{r^2 + a^2} + \frac{z^2}{r^2} = 1. \quad (116)$$

5. New Explanation To The Kerr-Schild Form

In the Kerr metric, the so-called Cartesian coordinates (x,y,z) are an axially symmetric spheroidal geometry and are also called the Kerr-Schild form. This geometry at a>0 does not pass through the origin x=y=z=0 and it shows the curvature singularity at r=0 and z=0. Using the terminology in

 doi:10.20944/preprints202109.0354.v2

differential geometry, this axially symmetric spheroidal geometry is a smooth manifold $N=\{(x,y,z)\in R^3|\}-\{(x,y)\in R^2|x^2+y^2=a^2,z=0\}$. In particular, the geometry, in this case, is not defined in the region $\{x^2+y^2<a^2,z=0\}$. They would not be appropriate coordinates to describe the things in the real world because it lacks the origin x=y=z=0 and a ring singularity exists. As we mentioned previously, if we apply the finite-size nuclear structure in the black hole, then this ring singularity at r=0 and θ=π /2 is naturally moved. Without imposing the pointlike concept, here a physical solution is adopted by using the finite-size nuclear structure and it satisfies the conservation of energy. At $r\to 0$ in the Boyer-Lindquist coordinates, we can choose enough small radius dr to enclose the point r=0, and in this enclosed region $0\le r\le dr$ we have

$$\lim_{r\to 0} m(r) \le \lim_{dr\to 0}\left\{\frac{4}{3}\pi(dr)^3 \max[\rho(0),\rho(dr)]\right\}=0, \tag{117}$$

where $\rho(r)$ is the mass density function at r and $\max[\rho(0),\rho(dr)]$ is the maximum of the mass density in this region. Then the conventional Kerr metric in this $m\to 0$ region becomes [29]

$$\begin{aligned} ds^2 \to dt^2 - \frac{r^2+a^2\cos^2\theta}{r^2+a^2}dr^2 - (r^2+a^2\cos^2\theta)d\theta^2 \\ -(r^2+a^2)\sin^2\theta d\phi^2, \end{aligned} \tag{118}$$

which is the flat Minkowski spacetime in the oblate spheroidal coordinates. Then we let the smooth manifold M described by the coordinates (r,θ,Φ) be another one, that is, $M=\{r\in[0,\infty),\theta\in[0,\pi],\phi\in[0,2\pi]\}-\{r=0,\theta=\pi/2\}$. It means that we have a map ξ projecting a point on the manifold M to the one on the manifold N, that is,

$$\xi:(r,\theta,\phi)\mapsto(x,y,z). \tag{119}$$

The inverse map can project a point on the Cartesian space back to the Boyer-Lindquist space, that is,

$$\xi^{-1}:(x,y,z)\mapsto(r,\theta,\phi). \tag{120}$$

In addition, the ring singularity in (x,y,z) is mapped to the singularity in (r,θ,Φ)

$$\xi:\{r=0,\theta=\pi/2\}\mapsto\{(x,y)\in R^2|x^2+y^2=a^2,z=0\}. \tag{121}$$

In fact, a similar concept also appears in this reference [24] where the family of confocal ellipsoids is mentioned. Explicitly speaking, this kind of singularity shall not appear in real space, and it is a mathematical singularity to be necessarily removed in the theory. Hence, we remove this kind of singularity in the theory by using a physical way, that is, the finite mass and charge density distributions in space. It is also similar when we deal with the Kerr-Newman metric later.

After the above discussions in previous section, then the Kerr-like metric by applying Equation (107) is [24]

$$ds^2=\left(1-\frac{2rGm(r)}{\rho^2c^2}\right)dt^2+\frac{4arGm(r)}{\rho^2c^2}\sin^2\theta dtd\phi-\frac{\rho^2}{\Delta}dr^2-\rho^2d\theta^2-\frac{\sin^2\theta}{\rho^2}[(r^2+a^2)^2-\Delta a^2\sin^2\theta]d\Phi^2, \tag{122}$$

where

$$\rho^2=r^2+a^2\cos^2\theta \tag{123}$$

and

$$\Delta=r^2-r\frac{2Gm(r)}{c^2}+a^2. \tag{124}$$

Therefore, we have the event horizons from the real solutions of the equation [24]

$$r_H^2+a^2-\frac{2Gr_Hm(r_H)}{c^2}=0. \tag{125}$$

It also gives a minimum mass value M_0 that two distinct event horizons exist at $M>M_0$ for the non-extremal black hole, a single degenerate event horizon at $M=M_0$ for the extremal black hole, and

 doi:10.20944/preprints202109.0354.v2

a black hole cannot be formed at $M<M_0$. One important thing is to consider the asymptotic form at $\theta=\pi/2$ and $r\to 0$ where the conventional Kerr metric exhibits the singularity ring. This asymptotic form leads to the rotating de Sitter geometry in which the Ricci curvature at the singular ring is [24]

$$\lim_{r\to 0^+} R(r,\theta=\pi/2)=\frac{4GM}{\sqrt{\pi}\vartheta^{3/2}c^2}. \tag{126}$$

It is the constantly finite curvature of the rotating de Sitter geometry. The singular ring in the conventional Kerr metric is replaced by a regular de Sitter, Saturn-like region of non-zero width in this Kerr-like metric so the mass source leads to a singularity-free metric to cure nonphysical features. In other words, the finite jump in curvature due to the de Sitter belt is instead of the conventional infinite discontinuity.

As $m\to 0$, the Kerr-like metric becomes the flat Minkowski spacetime in the oblate spheroidal coordinates

$$ds^2=\left(1-\frac{2rGm(r)}{\rho^2c^2}\right)dt^2+\frac{4arGm(r)}{\rho^2c^2}\sin^2\theta dtd\phi-\frac{\rho^2}{\Delta}dr^2-\rho^2d\theta^2 \\ -\frac{\sin^2\theta}{\rho^2}[(r^2+a^2)^2-\Delta a^2\sin^2\theta], \tag{127}$$

6. The Kerr-Newman-Like Metric And The Velocity Of Light In The Black Hole

There is other metric to discuss Einstein's spacetime structure, such as the traditional Kerr-Newman metric [10-15,20]. A singularity with infinite mass density at the center of the black hole is problematic as such that a lot of research would like to remove it. If we adopt a finite-size nucleus for a black hole, this mathematical singularity can disappear automatically. As mentioned previously [25], the Kerr-Newman-like metric removes a mathematical singularity at r=0 and $\theta=\pi/2$ from the traditional Kerr-Newman metric [25]. This has been reasonably explained in Sec. 4 and Sec. 5. On the other hand, the accretion disc is made up of a lot of plasma and electrons, so the materials that the black hole swallows contain positively and negatively electric substances very often, and it is difficult to maintain a black hole electrically neutral at any time. Therefore, it is a more reasonable choice to consider rotating and charged black holes. In Equation (127), the Kerr-Newman-like metric with a finite-size nucleus [25] is a more appropriate way to describe the spacetime at the rotating and charged black hole. About the rotating charged black hole, using the Newman-Janis algorithm in the Boyer-Lindquist coordinates, the line element of a Kerr-Newman-like metric [25] similar to Equation (52) is

$$ds^2=\frac{\Delta-a^2\sin^2\theta}{\rho^2}c^2dt^2-\frac{\rho^2}{\Delta}dr^2-\rho^2d\theta^2+2ac\sin^2\theta\left(1-\frac{\Delta-a^2\sin^2\theta}{\rho^2}\right)dtd\phi \\ -\left[\rho^2+a^2\sin^2\theta\left(2-\frac{\Delta-a^2\sin^2\theta}{\rho^2}\right)\right]\sin^2\theta d\phi^2, \tag{128}$$

in which ρ^2 is the same definition as Equation (123) and Δ is similar to the one in Equation (124), but r-dependent on R_S and R_Q, that is,

$$\Delta(m,q)=r^2-r\frac{2Gm(r)}{c^2}+a^2+\frac{KG}{c^4}q(r)^2, \tag{129}$$

where

$$q(r)^2=\frac{Q^2}{\pi}\left[\gamma^2\left(\frac{1}{2};\frac{r^2}{4\vartheta}\right)-\frac{r\gamma\left(\frac{1}{2};\frac{r^2}{2\vartheta}\right)}{\sqrt{2\vartheta}}+\sqrt{\frac{2}{\vartheta}}r\gamma\left(\frac{3}{2};\frac{r^2}{4\vartheta}\right)\right]. \tag{130}$$

This Kerr-Newman-like metric also results in three possible situations including the nonextremal black hole exists with two distinct event horizons at $M>M_0$, an extremal black hole with

 doi:10.20944/preprints202109.0354.v2

a single degenerate event horizon at M=M_0, and no black hole at M<M_0 [25]. In this metric, the coordinate time t in the Kerr-Newman-like metric is also the time read by the clock stationed at infinity because the proper time and coordinate time become identical [14]. The velocity of light is ds^2=0, and using Equation (127), we have the velocity equation of light in terms of (dr/dt, rdθ/dt, $r$sinθdϕ/dt)

$$\frac{\rho^4}{\Delta(m,q)[\Delta(m,q)-a^2\sin^2\theta]}\left(\frac{\mathrm{d}r}{dt}\right)^2+\frac{\rho^4}{r^2[\Delta(m,q)-a^2\sin^2\theta]}\left(r\frac{\mathrm{d}\theta}{\mathrm{d}t}\right)^2 - \frac{[\Delta(m,q)a^2\sin^2\theta-(r^2+a^2)^2]}{r^2[\Delta(m,q)-a^2\sin\theta]}\left(r\sin\theta\frac{\mathrm{d}\phi}{dt}\right)^2 - \frac{2ac[-\Delta(m,q)+(r^2+a^2)]\sin\theta}{r[\Delta(m,q)-a^2\sin^2\theta]}\left(r\sin\theta\frac{\mathrm{d}\phi}{dt}\right)=c^2. \quad (131)$$

Then we can build the connection between the reasonable speed of light and the proposed nuclear structure.

Similar to Equation (2), Equation (131) gives the relationship between three velocity components of light (dr/dt, rdθ/dt, $r$sinθdϕ/dt) in the Kerr-Newman-like metric. The appropriate and reasonable way to use Equation (131) is that each velocity component is real and finite. We have discussed the velocity of light for the rotating and charged black hole [44,68]. Especially, if we want to discuss light propagating into a black hole, the radial speed of light at the event horizon must be nonzero. By Equation (131), the radial velocity v_r of light propagating along the radial direction at the black hole is

$$v_r=\frac{dr}{dt}=\pm\frac{\rho^2}{\sqrt{\Delta(m,q)[\Delta(m,q)-a^2\sin^2\theta]}}c. \quad (132)$$

In actual physical phenomena, it requires the radial velocity real, nonzero, and non-complex everywhere. Two solutions are given in Equation (132) [20], one is forward and the other is backward the event horizon. Thus, the denominator in Equation (132) has to be real and the first condition is

$$r^2-r\frac{2Gm(r)}{c^2}+\frac{G^2m(r)^2}{c^4}+a^2+\frac{KGq(r)^2}{c^4}-\frac{G^2m(r)^2}{c^4}>0, \quad (133)$$

and

$$r^2-r\frac{2Gm(r)}{c^2}+\frac{G^2m(r)^2}{c^4}+a^2\cos^2\theta+\frac{KGq(r)^2}{c^4}-\frac{G^2m(r)^2}{c^4}>0. \quad (134)$$

The other condition is

$$r^2-r\frac{2Gm(r)}{c^2}+\frac{G^2m(r)^2}{c^4}+a^2+\frac{KGq(r)^2}{c^4}-\frac{G^2m(r)^2}{c^4}<0, \quad (135)$$

and

$$r^2-r\frac{2Gm(r)}{c^2}+\frac{G^2m(r)^2}{c^4}+a^2\cos^2\theta+\frac{KGq(r)^2}{c^4}-\frac{G^2m(r)^2}{c^4}<0. \quad (136)$$

However, in Equation (127), the time transfer between the local reference frame and the far-away reference frame is

$$ds^2=\frac{\Delta-a^2\sin^2\theta}{\rho^2}c^2dt^2, \quad (137)$$

and it has to be positive. According to this, the second condition in Equation (136) is unsatisfied anymore. Hence, at any position r, it requires

 doi:10.20944/preprints202109.0354.v2

$$a^2\cos^2\theta + \frac{KGq(r)^2}{c^4} - \frac{G^2m(r)^2}{c^4} > 0, \quad (138)$$

In the equatorial plane where $\theta = \pi/2$, it more strictly requires

$$Kq(r)^2 > Gm(r)^2. \quad (139)$$

If the above condition is satisfied, then we can find real and finite solutions for Equation (132) to describe the radial speed of light in the rotating and charged black hole. Based on this model, the speed of light observed at far-away places can be nonzero at the event horizon. The discussion of the radial speed of light predicts the expansion of the black hole to be observable.

7. Conclusion

In summary, the reasonableness of the singularity of the black hole is studied in this paper. When we consider that everything in the black hole collects at a singularity, the infinite density of mass, charge, gravitational energy, and electric energy would be very nonphysical. Does it give rise to a curiosity about why all masses, as well as all charges, gather at a point? However, the black hole is very possibly evolutional from a star with finite energy. Such a structure doesn't obey energy conservation. If we believe in the singularity in the black hole, we just believe in the knowledge in the 1920s or 1930s, one hundred years ago. At that age, people still had no deep ideas about neutrons, they even didn't know what the strong interaction and quarks are. They just treated a mathematical solution as a real physical object without any believable proof of its physical truth. When we put the black hole and the Big Bang together, we will see very clearly that singularity is just a contradictory concept. The ultra-super strong gravity of the singularity before the Big Bang will affect the explosion and stop the expansion of the universe.

About singularity, an example of the degenerate Fermi electron gas is used to check whether the singularity exists or not. It clearly shows that no matter how large the energy of the Fermi electron gas is, those electrons cannot shrink to a point, physically speaking. They always have finite volumes discussed in statistical mechanics. The singularity also tells us that gravitational energy and Coulomb's energy are infinite there. Since a lot of black holes are evolutionary from stars with finite energy, it is unreasonable to have infinite energy for black holes. We also use a case of $1.4\text{x}10^{31}$ Coulomb electrons at infinity to demonstrate that to collect those electrons in a sphere with a radius of 50 meters needs to do a work of $2.114\text{x}10^{70}$ Joules, which is more than the energy in the observable universe. In such a case, the distance between two electrons is larger than 10^{-15} meter whereas classical electrodynamics is still useful. This case tells us that the traditional concept of gravitational collapse cannot shrink those electrons to be a singularity, and the process of the collection is physical. We have to input a lot of energy to gather those electrons in a small space. Hence, the charged sources described by the Kerr or Kerr-Newman metrics are not easily small in space because Coulomb's force is against the shrinking process. Then we use the neutron gas as the most possible constituents after a supernova to discuss their volume based on energy conservation. The result also tells us a similar result as we have already known in the Fermi electron gas. So theoretically speaking, a black hole has a finite-size nucleus inside it, not a singularity.

One important thing in this paper is that a complex structure of a double-characteristic black hole is proposed where the total charge can be zero or nonzero. This kind of black hole has a positively charged region I, possibly consisting of protons, which is covered by neutral thin Region II such as neutrons. Their outmost thin layer consists of electrons. We follow the report that a charged and non-rotating compact star with a mass of solar mass and a radius of $0.9367Rs$ can have a charge as high as $1.648824\text{x}10^{20}$ Coulombs. Adopting these quantities in our model, the spacetime in Region I and Region II is described by the Reissner–Nordström metric. Within the outmost layer, the spacetime is described by the Kerr–Newman metric, and the place outside the outmost layer is also described by the Kerr-Newman metric. The counter-rotating and corotating electrons in Region III can make the whole structure charged or uncharged, and rotating or non-rotating. Some allowed radii of the counter-rotating and corotating electrons are given to reach the whole structure within

 doi:10.20944/preprints202109.0354.v2

the outer event horizon of the Kerr-Newman black hole. Due to this structure, it reaches $r_+ \geq \max(r_1, r_2)$ so the black hole is formed by our model. A simple case gives a Schwarzschild black hole when both the counter-rotating and corotating electrons are equal, move on very close orbitals, and the total charge of the whole structure is zero. In such a case, a finite-size structure in the Kerr–Newman metric transforms into a Schwarzschild black hole. To sum up, our model can construct black holes, and the properties of the black holes are dominated by the corotating and counter-rotating electrons, which make the black holes charged or uncharged, and rotating or non-rotating.

Finally, from the Kerr-Newman metric, we build the relationship of the three velocity components at each point for light in the black hole. If the singularity is replaced with the finite-size nucleus in the black hole, then the mathematical singularity in the Kerr-Newman metric at r=0 and $\theta = \pi/2$ automatically disappears. For the special case of a=0 and R_Q=0, it tells us that there are two solutions for the radial speed at the Schwarzschild radius. Especially, the investigations of gravitational waves from binary black holes reveal that gravitational waves can escape black holes away from their inside [5-8]. Theoretically speaking, both light and the gravitational wave follow the same spacetime structure at the black hole and their trajectories are null geodesic. It means that light should escape the black hole. Furthermore, based on this finite-nucleus model, the speed of light observed at far-away places can be nonzero at the event horizon. The discussion of the radial speed of light predicts the expansion of the black hole to be observable.

Data Availability Statement: All data that support the findings of this study are included within the article.

Acknowledgement: This research is under no funding.

References

1. Makoto Miyoshi, James Moran, James Herrnstein, Lincoln Greenhill, Naomasa Nakai, Philip Diamond, Makoto Inoue, "Evidence for a black hole from high rotation velocities in a sub-parsec region of NGC4258," Nature **373**, 127 (1995).
2. J. M. Miller, J. Raymond, C. S. Reynolds, A. C. Fabian, T. R. Kallman, and J. Homan, "The Accretion Disk Wind In The Black Hole GRO J1655-40," The Astrophysical Journal **680**, 1359 (2008).
3. I. M. McHardy, K. F. Gunn, P. Uttley, and M. R. Goad, "MCG–6-30-15: long time-scale X-ray variability, black hole mass and active galactic nuclei high states," Mon. Not. R. Astron. Soc. **359**, 1469 (2005).
4. Pieter van Dokkum et al., "A Candidate Runaway Supermassive Black Hole Identified by Shocks and Star Formation in its Wake," *Astrophy. J. Lett.* **946**, L50 (2023).
5. B. P. Abbott et. al. (LIGO Scientific Collaboration and Virgo Collaboration), "Observation of Gravitational Waves from a Binary Black Hole Merger," Phys. Rev. Lett. **116**, 061102 (2016).
6. B. P. Abbott et al. (LIGO Scientific Collaboration and Virgo Collaboration), "GW151226: Observation of Gravitational Waves from a 22-Solar-Mass Binary Black Hole Coalescence," Phys. Rev. Lett. **116**, 241103 (2016).
7. B. P. Abbott et al. (LIGO Scientific Collaboration and Virgo Collaboration), "GW170104: Observation of A 50 Solar-Mass Binary Black Hole Coalescence at Redshift 0.2," Phys. Rev. Lett. **118**, 221101 (2017).
8. B. P. Abbott et al. (LIGO Scientific Collaboration and Virgo Collaboration), "GW170814: a Three-Detector Observation of Gravitational Waves from A Binary Black Hole Coalescence," Phys. Rev. Lett. **119**, 141101 (2017).
9. B. P. Abbott et al. (LIGO Scientific Collaboration and Virgo Collaboration), "GW170817: Observation of Gravitational Waves from A Binary Neutron Star Inspiral," Phys. Rev. Lett. **119**, 161101 (2017).
10. Bernard F. Schutz, *A First Course In General Relativity* (Cambridge University Press, Cambridge, 1985), P.291.
11. Hans C. Ohanian and Remo Ruffini, *Gravitation and Spacetime* (W. W. Norton & Company, 2nd ed., New York, 1994), P.445 & P. 449.
12. F. De Felice & C. J. S. Clarke, *Relativity On Curved Manifolds* (Cambridge University Press, Cambridge, 1990), P.355 & P.362.
13. Hans Stephani, *Relativity-An Introduction To Special And General Relativity* (Cambridge, 3rd ed., Cambridge, 2004), P.303.
14. Richard A. Mould, *Basic Relativity* (Springer, New York, 2002), P.324.
15. Charles W. Misner, Kip S. Thorne, and John Archibald Wheeler, *Gravitation* (W. H. Freeman and Company, 1970), P.880.
16. The Event Horizon Telescope Collaboration et. al., "First M87 Even Horizon Telescope Results. I. The Shadow of the Supermassive Black Hole," *Astrophys. J. Lett.* **875**, L1 (2019).

17. 17 Tal Alexander and Priyamvada Natarajan, "Rapid Growth of Seed Black Holes in The Early Universe by Subra-Exponential Accretion," Sci. **345**, 1330 (2014).
18. Muhammad A. Latif and Andrea Ferrara, "Formation of Supermassive Black Hole Seeds," Publications of the Astronomical Society of Australia **33**, e051 (2016).
19. Angelo Ricarte and Priyamvada Natarajan, "The Observable Signatures of Massive Black Hole Seeds," *Mon. Not. Roy. Astro. Soc.* **481**, 3278-3292 (2018).
20. Tim Adamo and E.T. Newman, "The Kerr-Newman Metric: A Review." arXiv: 1410.6626 (2014).
21. P. Nicolini, "A Model of Radiating Black Hole in Noncommutative Geometry," *J. Phys. A: Math. Gen.* **38** (2005) L631–L638. doi:10.1088/0305-4470/38/39/l02
22. P. Nicolini, A. Smailagic, and E. Spallucci, "Noncommutative Geometry Inspired Schwarzschild Black Hole," *Phys. Lett. B* **632** (2006) 547–551. doi:10.1016/j.physletb.2005.11.004
23. S. Arsodi, P. Nicolini, A. Smailagic, and E. Spallucci, "Non-Commutative Geometry Inspired Charged Black Hole," *Phys. Lett. B* **645** (2007) 261–266.
24. A. Smailagicand E. Spallucci, "'Kerrr" Black Hole: The Lord of the String," *Phys. Lett. B* **688** (2010) 82–87. doi:10.1016/j.physletb.2010.03.075
25. L. Modesto and P. Nicolini, "Charged Rotating Noncommutative Black Holes," *Phys. Rev. D* **82** (2010) 104035–14. doi:10.1103/physrevd.82.104035
26. E. Spallucci, A. Smailagic, and P. Nicolini, "Non-Commutative Geometry Inspired High-Dimensional Charged Black Holes," *Phys. Lett. B* **670** (2009) 449-454.
27. Nicolini and E. Spallucci, "Non-Commutative Geometry Inspired Dirty Black Holes," Classical and Quantum Gravity **27** (2009) 015010.
28. Piero Nicolini, "Non-commutative Black Holes, The Final Appeal to Quantum Gravity: A Review," *Int. J. Mod. Phys. A* **24** (2009) 1229-1308.
29. Matt Visser. The Kerr Spacetime: A Brief Introduction. https://arxiv.org/pdf/0706.0622.pdf
30. G. Venkataraman, (1992). *Chandrasekhar and his limit*, (Universities Press, India), P.89.
31. Ting-Hang Pei, "The Highly Accurate Relation Between Radius and Mass of The White Dwarf Star from Zero to Finite Temperature," *Front. Astro. Space Sci.*, 01 February 2022. doi.org/10.3389/fspas.2021.799210
32. J. R. Oppenheimer and G. M. Vokff, "On Massive Neutron Core," Physics Review **55**, 374, (1939).
33. Henning Heiselberg and Vijay Pandharipande, "Recent Progress in neutron Star Theory" (2000). https://arxiv.org/abs/astro-ph/0003276
34. Vassiliki Kalogera and Gordon Baym, "The Maximum Mass of A Neutron Star," *Astrophys. J.* **470**, L61-L64 (1996).
35. V. D. Burkert, L. Elouadrhiri, and F. X. Girod, "The Pressure Distribution inside the Proton," *Nat.* **557** (2018) 396–399. doi:10.1038/s41586-018-0060-z
36. M. Fukugita and P. J. E. Peebles, "The Cosmic Energy Inventory," *Astrophys. J.* **616** (2004) 643–68.
37. Richard P. Feynman, Robert B. Leighton, and Matthew Sands, The Feynman Lectures on Physics – The New Millennium Edition - Volume II: Mainly Electromagnetism and Matter (1964, California Institute of Technology), P.5-7.
38. J. D. V. Arbañil, J. P. S. Lemos, and V. T. Zanchin, "Incompressible relativistic spheres: electrically charged stars, compactness bounds, and quasiblack hole configurations," Phys. Rev. D **89**, 104054 (2014).
39. José P. S. Lemos, Francisco J. Lopes, Gonçalo Quinta, and Vilson T. Zanchin, "Compact stars with a small electric charge: the limiting radius to mass relation and the maximum mass for incompressible matter," *Eur. Phys. J. C* **75**, 76 (2015).
40. M. Sharif and Iqra Ijaz Butt, "Complexity Factor for Charged Spherical System," Eur. Phys. J. C **78**, 688 (2018).
41. M. K. Jasim, S.K. Maurya, Saibal Ray, Dibyendu Shee, Debabrata Deb, Farook Rahaman, "Charged Strange Stellar Model Describing by Tolman V Metric," Results in Physics **20**, 103648 (2021).
42. Subharthi Ray, Aquino L. Espíndola, and Manuel Malheiro," Electrically Charged Compact Stars and Formation of Charged Black Holes," Phys. Rev. D **68**, 084004 (2003).
43. S. K. Maurya, Ayan Banerjee, and Phongpichit Channuie, "Relativistic Compact Stars with Charged Anisotropic Matter," Chinese Phys. C **42**, 055101 (2018).
44. Ting-Hang Pei, "The Superluminal Phenomenon of Light near The Kerr-Newman Black Hole or Super-Gravitational Source," *Front. Phys.* **9**, 701619 (2021).
45. https://doi.org/10.3389/fphy.2021.701619
46. Kerson Huang, *Statistical Mechanics* (John Weily & Sons, Inc., 2nd, 1987), P.247.
47. Walter Greiner, Ludwig Neise, and Horst Stocker, *Thermodynamics and Statistical Mechanics* (Springer, New York, 1995), p.355.
48. Arieh Sher, "Is A Black Hole A Neutron Star?" http://vixra.org/abs/1806.0329.
49. S. M. de Carvalho, M. Rotondo, Jorge A. Rueda, and R. Ruffini, "The Relativistic Feynman-Metropolis-Teller Treatment at Finite Temperatures," Phys. Rev. C **89**, 015801 (2014).

50. K. A. Boshkayev, J. A. Rueda, B. Zhami, Zh. A. Kazymova, and G. Sh. Balgymbekov, "Equilibrium Structure of White Dwarfs at Finite Temperatures," International Journal of Modern Physics: Conference Series **41**, 1660129 (2015).
51. R. V. Lobato, G. A. Carvalho, N. G. Kelkar, and M. Nowakowski, "Mssive White Dwarfs in $f(R,L_m)$ gravity," Eur. Phys. J. C **82**, b540 (2022).
52. James M. Lattimer, "The Nuclear Equation of State and Neutron Star Masses," Annu. Rev. Nucl. Part. Sci. **62**, 485–515 (2012).
53. A. W. Steiner, J. M. Lattimer, and E. F. Brown, "Neutron Star Radii, Universal Relation, and the Role of Prior Distributions," Eur. Phys. J. A **52**, 18 (2016).
54. Feryal Özel and Dimitrios Psaltis, "Reconstructing The Neutron-Star Equation of State from Astrophysical Measurements," Phys. Rev. D **80**, 103003 (2009).
55. Jocelyn S. Read, Benjamin D. Lackey, Benjamin J. Owen, and John L. Friedman, "Constraints on A Phenomenologically Parametrized Neutron-Star Equation of State," Phys. Rev. D **79**, 124032 (2009).
56. Rodrigo Pican¸co Negreiros, Fridolin Weber, Manuel Malheiro, and Vladimir Usov, "Electrically Charged Strange Quark Stars," Phys. Rev. D **80**, 083006 (2009).
57. Baiju Dayanandan, S.K. Maurya, and Smitha T. T, "Modelling of Charged Anisotropic Compact Stars in General Relativity," Eur. Phys. J. A **53,** 141 (2017).
58. Satyanarayana Gedela, Neeraj Pant, Jaya Upreti, and R. P. Pant, "A New Parametric Class of Solutions of A Charged Anisotropic Compact Star via Bardeen Exterior Geometry," Modern Physics Letter A **36**, 2150055 (2021).
59. Juan M. Z. Pretel, Ayan Banerjee, and Anirudh Pradhan, "Electrically Charged Quark Stars in 4D Einstein-Gauss-Bonett Gravity," Eur. Phys. J. C **82**, 180 (2022).
60. Ting-Han Pei, "The Additional Pressure of White Dwarf Stars Generated by Net Charges," The Publications of the Astronomical Society of Japan **75**, 893-906 (2023).
61. Håkan Andréasson, "Sharp bounds on the critical stability radius for relativistic charged spheres," Communications in Mathematical Physics **288**, 715-730 (2009).
62. M. K. Jasim, S. K. Maurya, Saibal Ray, Dibyendu Shee, Debabrata Deb, and Farook Rahaman, "Charged strange stellar model describing by Tolman *V* metric," Results in Physics **20**, 103648 (2021).
63. G. Estevez-Delgado, J. Estevez-Delgado, M. Pineda Duran, N. Montelongo Garc´ıa, and J.M. Paulin-Fuentes, "A charged perfect fluid model with high compactness," Revista Mexicana de F´ısica **65**, 382–391 (2019).
64. Jiri Bicak, Zdenek Suchlik, and Vladimir Balek, "The motion of charged particles in the field of rotating charged black holes and naked singularities," *Astronomical Institutes of Czechoslovakia, Bulletin* **40**, 65-92 (1989).
65. Vladimir Balek, Jiri Bicak, and Zdenek Stuchlik, "The motion of the charged particles in the field of rotating charged black holes and naked singularities. II-The motion in the equatorial plane," *Astronomical Institutes of Czechoslovakia, Bulletin* **40**, 133-165 (1989).
66. Eva Hackmann and Hongxiao Xu. "Charged particle motion in Kerr-Newman space-times." *Physical Review D* **87**, 124030 (2013).
67. Shanjit Heisnam, Irom Ablu Meitei, and Kangujam Yugindro Singh, "Motion of a Test Particle in the Kerr-Newman De/Anti De Sitter Space-Time," *International Journal of Astronomy and Astrophysics* **4**, 365-373 (2014).
68. Hakan Cebeci, Nülifer Özdemir, and Seçil Şentorun, "The Equatorial Motion of Charged Test Particles in Kerr-Newman-Taub-NUT Spacetime," General Relativity and Gravitation **51**, 84 (2019).
69. Ting-Hang Pei, "The Average Radial Speed of Light From Near to Far Space Surrounding the Kerr–Newman Super-Gravitational Source," Frontiers in Astronomy and Space Sciences **9**, 878156 (2022).
70. Daniela Pugliese, Hernando Quevedo, and Remo Ruffini, "Equatorial circular orbits of neutral test particles in the Kerr-Newman spacetime, " *Physical Review D* **88**, 024042 (2013).
71. Chen-Yu Liu, Da-Shin Lee, and Chi-Yong Lin, "Geodesic motion of neutral particles around a Kerr–Newman black hole," *Classical and Quantum Gravity* **34**, 235008 (2017).
72. Parthapratim Pradhan, "Circular geodesics in the Kerr–Newman–Taub–NUT spacetime," *Classical and Quantum Gravity* **32**, 165001 (2015).
73. Felipe J. Llanes-Estrada, Gaspar Moreno Navarro, "Cubic Neutrons," Mod. Phys. Lett. A **27** (2012) 1250033.
74. Pedro Calvo Portela, Felipe J. Llanes-Estrada, "Cubic Wavefunction Deformation of Compressed Atoms," Few-Body Syst. **56** (2015) 231.
75. *Mark G. Alford, Andreas Schmitt, Krishna Rajagopal, and Thomas Schäfer*, "Color Superconductivity in Dense Quark Matter," Rev. Mod. Phys. **80**, 1455 *(2008).*
76. Kenji Fukushima and Tetsuo Hatsuda, "The Phase Diagram of Dense QCD," Rep. Prog. Phys. **74**, 014001 (2011).

 doi:10.20944/preprints202109.0354.v2

disclaim responsibility for any injury to people or property resulting from any ideas, methods, instructions or products referred to in the content.